



MODELING CONNECTIVITY: DCM for EEG

Rosalyn Moran
Department of Neuroimaging,
IOPPN
King's College London

16/09/2021, ETH Zurich
Computational Psychiatry Course 2021

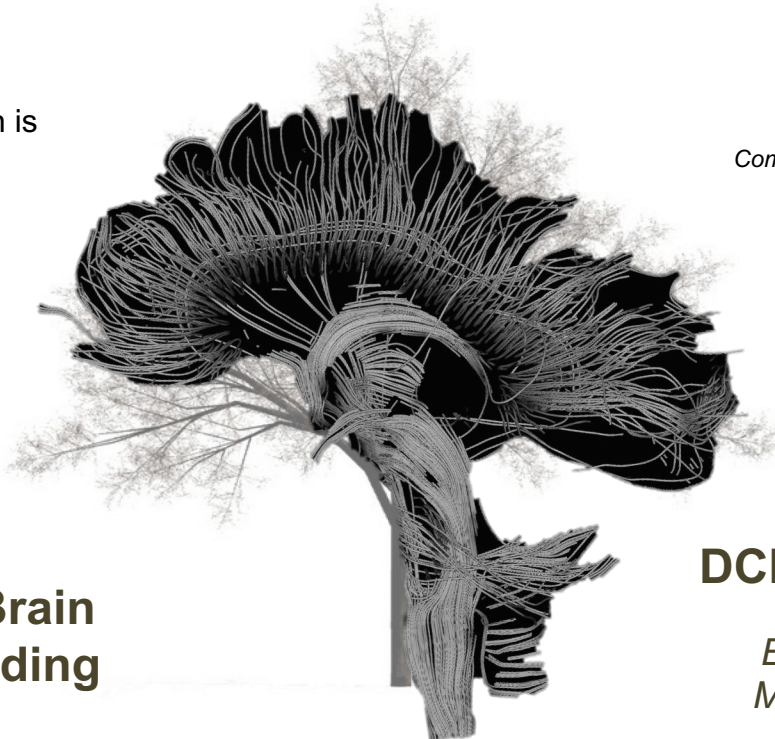
Models of the Brain

“Normative models describe how an optimal system would work given the goals. They describe ‘what’ the brain is trying to do.”



The Bayesian Brain & Predictive Coding

Computational Understanding of the Brain’s ‘thought algorithms’



“Process models are about the mechanisms, thus describing ‘how’ it is done.”

Computational Psychiatry, Gordon et al, MIT Press



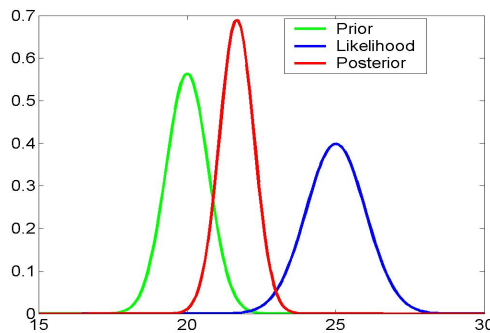
DCM & Brain Connectivity

Biological Models to Measure Connectivity

Theoretical Models of Brain Function



Thomas Bayes 1701-1759



"The general rule according to which visual representations determine themselves ... is that we *always find* present in the visual field such objects as would have to exist in order for them to produce the same impression on the neural apparatus under the *usual normal conditions* of the use of our eyes."

Hermann von Helmholtz (1821 - 1894) *Perception as Inference*

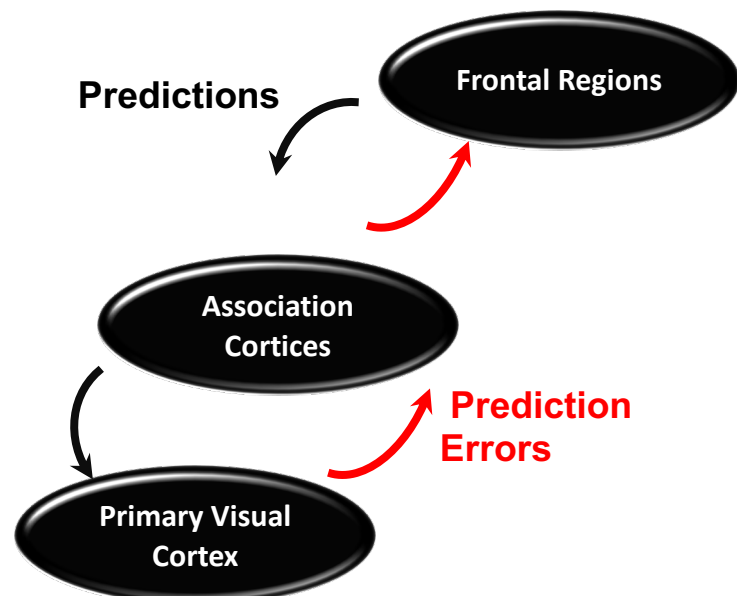
Dayan, Hinton, Neal & Zemel (1995) **The Helmholtz Machine**

Montague, Dayan, Sejnowski (1996) **Dopamine Systems Signal Reward Prediction Errors**

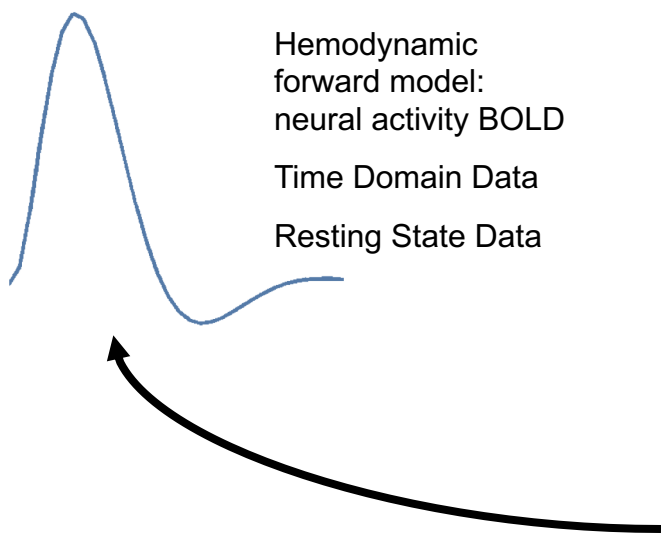
Rao & Ballard (1999) **Predictive coding in the visual cortex**

Friston (2010) **The free-energy principle: a unified brain theory?**

Moran et al. (2012) **Neuromodulators in Predictive Coding**



Dynamic Causal Modeling: Generic Framework

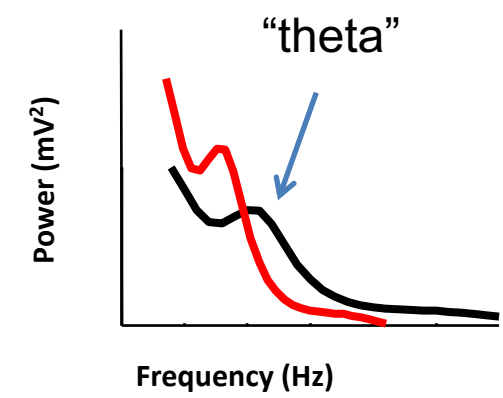


Electromagnetic forward model:
neural activity EEG
MEG
LFP

Time Domain ERP Data
Phase Domain Data
Time Frequency Data
Spectral Data

Neural state equation:

$$\frac{dx}{dt} = F(x, u, \theta)$$

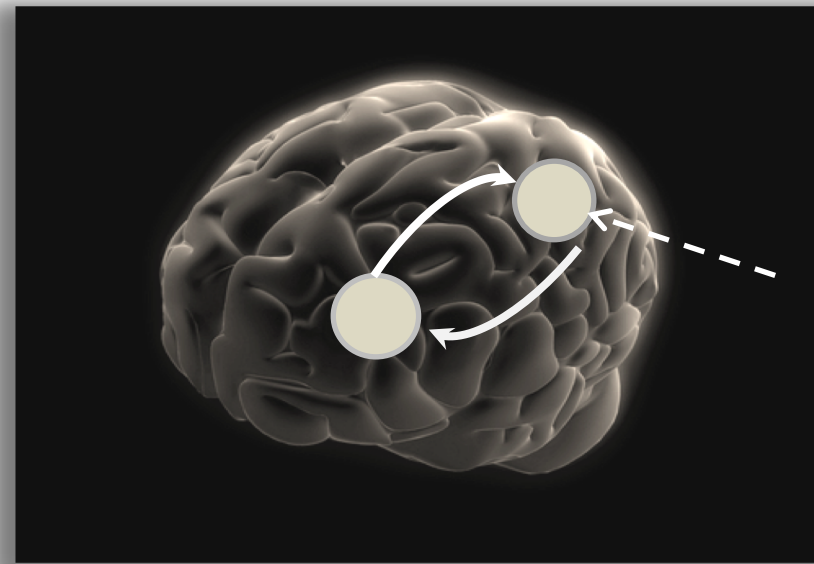


fMRI

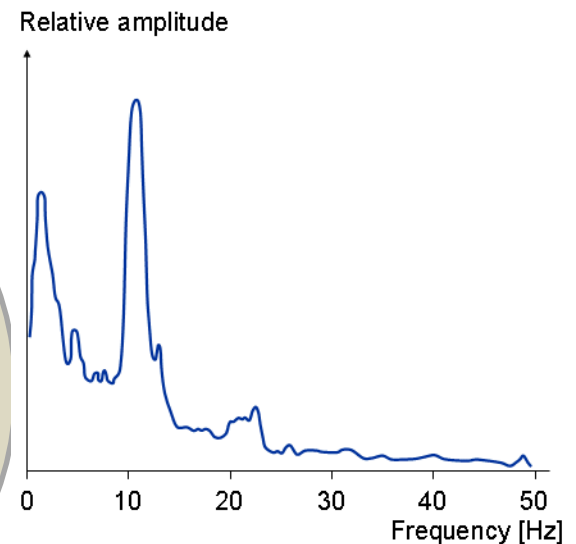
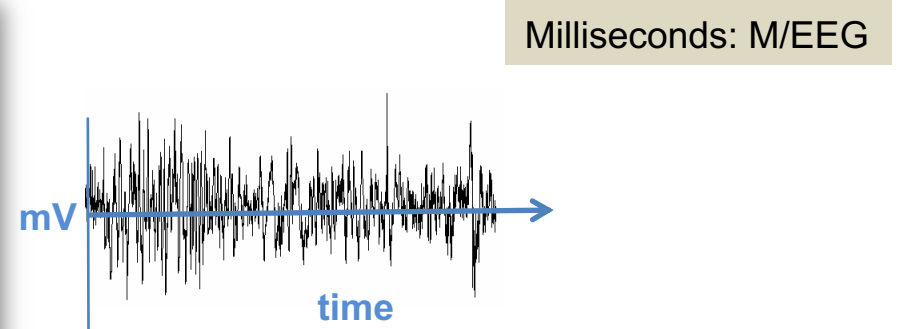
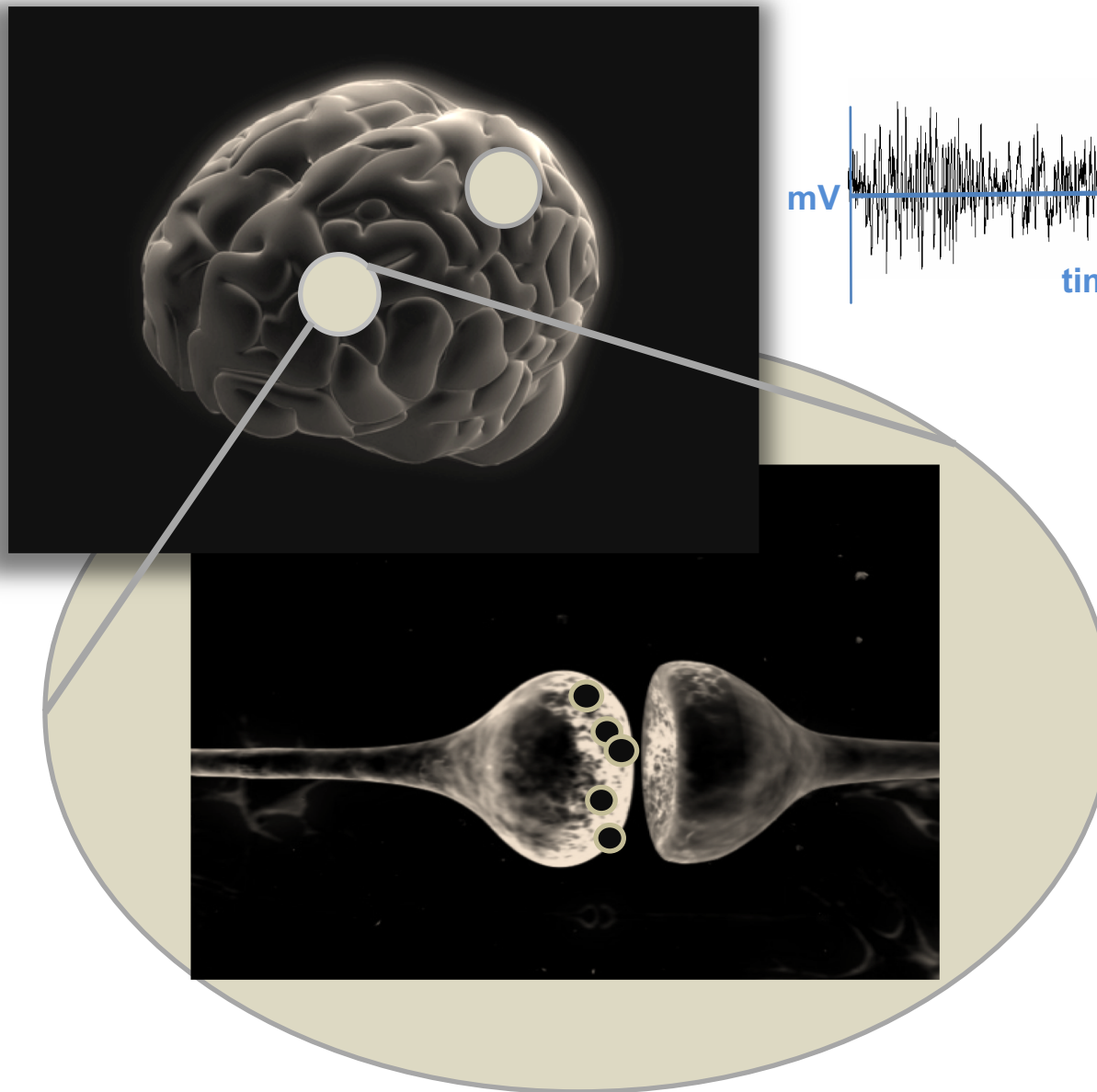
simple neuronal model
(slow time scale)

EEG/MEG

detailed neuronal model
(synaptic time scales)



Connectivity from EEG/LFP Data: Dynamic Causal Models



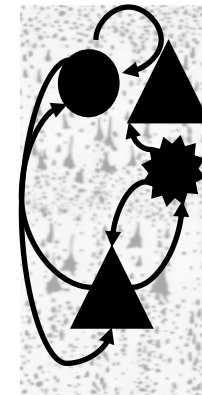
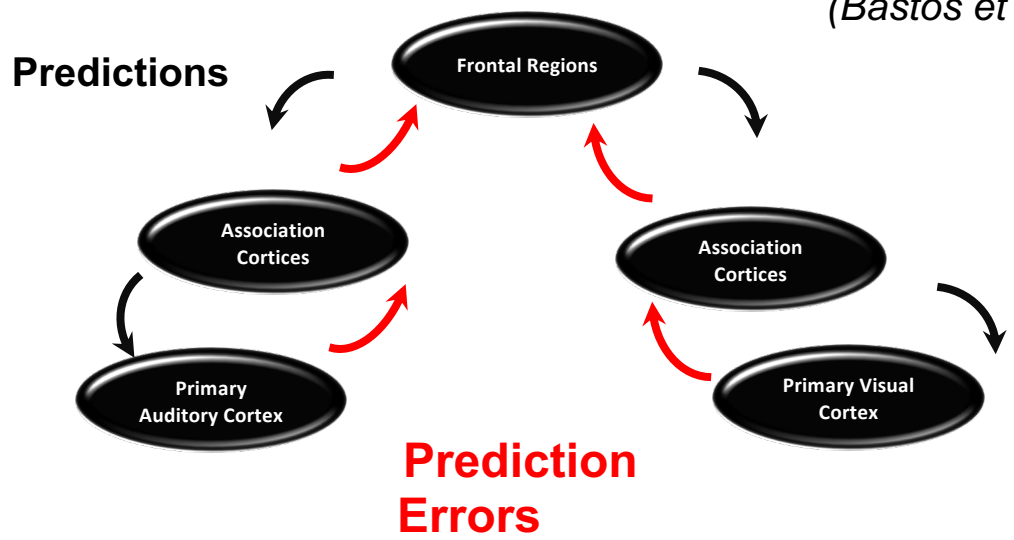
Hippocampal Theta (4 – 8 Hz)
Sensory Gamma (30 – 60 Hz)
Motor Beta (16-32 Hz)

Generative Models of Brain Connectivity via DCM

A canonical microcircuit for neocortex, Douglas, Martin & Whitteridge, 1989

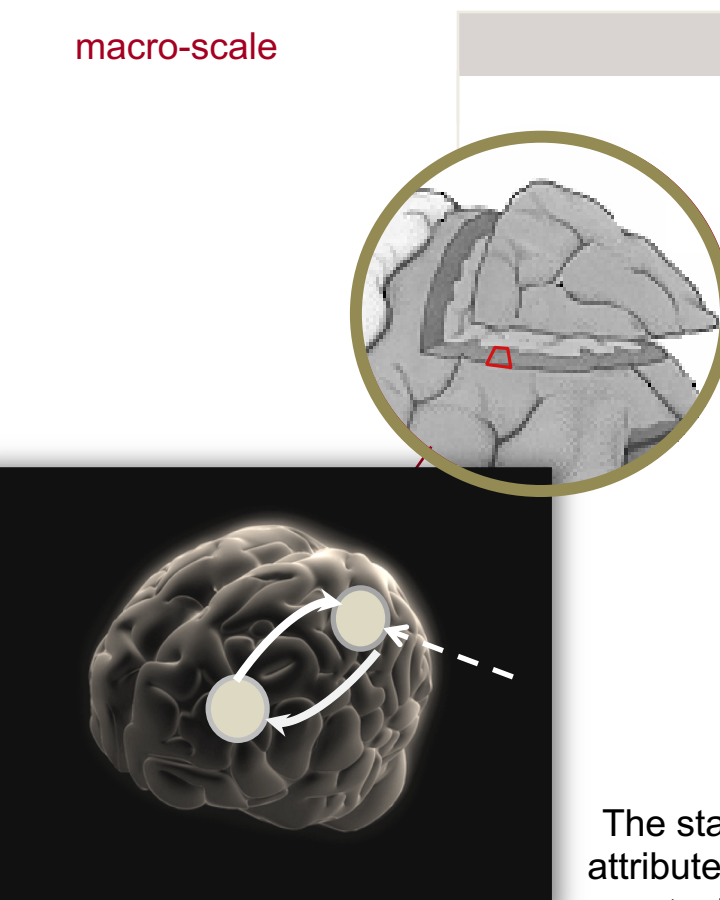
“...The circuit explains ...three basic populations of neurons, and reveals the following features ...important to computational theories of neocortex. First, inhibition and excitation are not separable events. ...Second, **the thalamic input does not provide the major excitation arriving at any neuron**. Instead the intracortical excitatory connections provide most of the excitation. Third, the time evolution ...far longer than the synaptic delays of the circuits involved.”

DCM & Canonical Microcircuits (Bastos et al 2012)

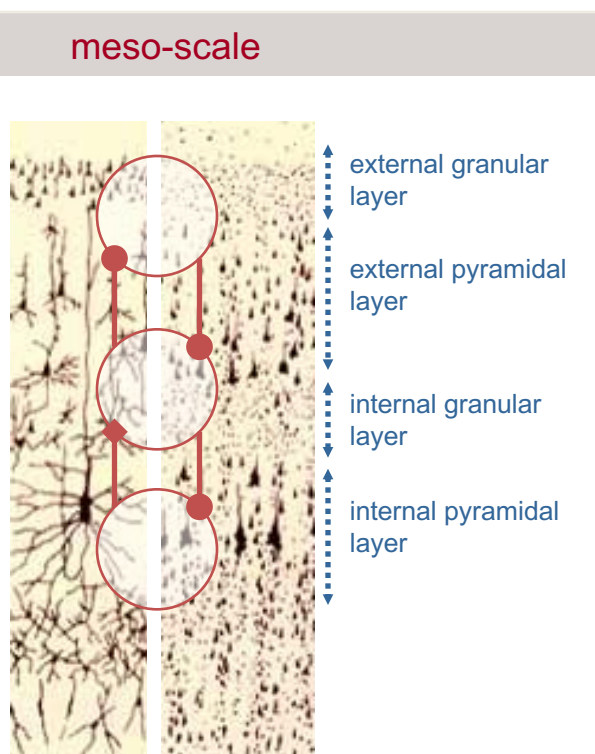


Macro and meso-scales: The Neural Mass Model

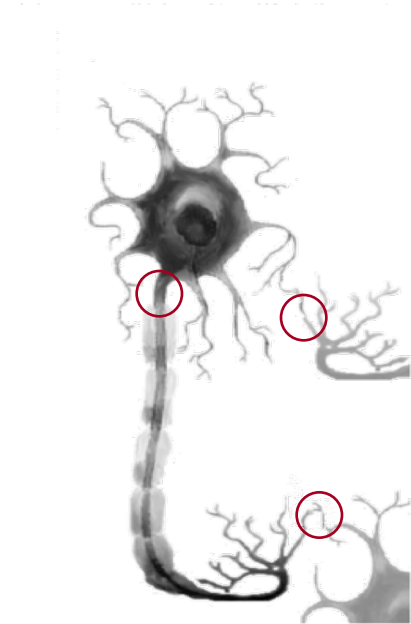
macro-scale



meso-scale

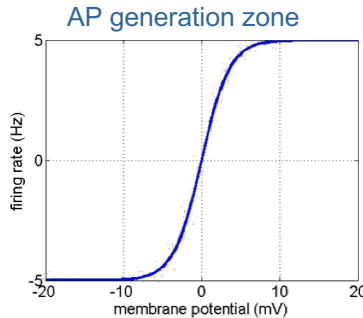


micro-scale

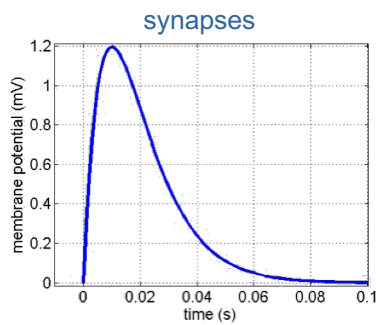


The state of a neuron comprises a number of attributes, membrane potentials, conductances etc. Modelling these states can become intractable. **Mean field approximations** summarise the states in terms of their ensemble density. **Neural mass models** consider only point densities and describe the interaction of the means in the ensemble

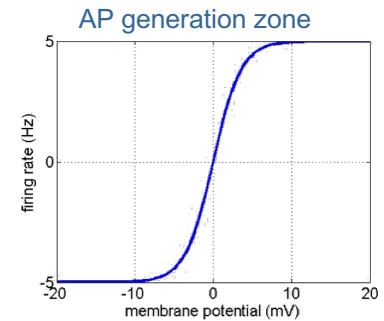
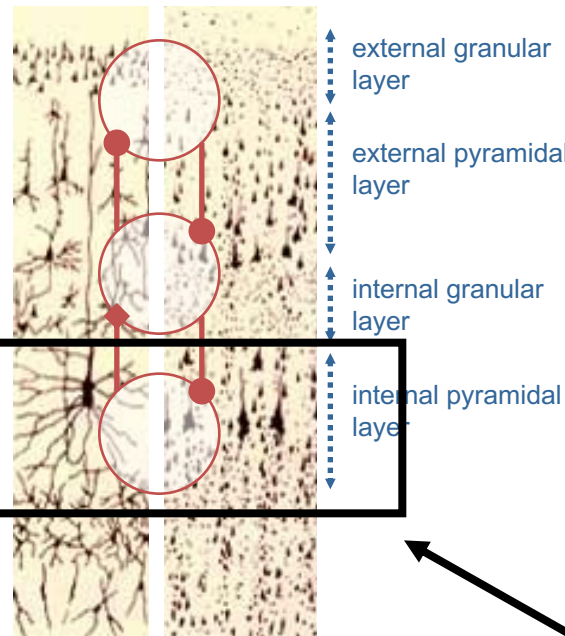
Meso-scale dynamics



$\theta(2)$



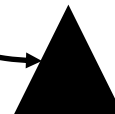
$\theta(1)$



Convolution Based Neural Mass Models

Convolution-Based Neural Mass Models in DCM

Spiny stellate cells



Pyramidal cells

$$v_{post} = \sigma(v_{pre}) \otimes h$$

Take one spiny stellate cell.....

Convolution-Based Neural Mass Models in DCM

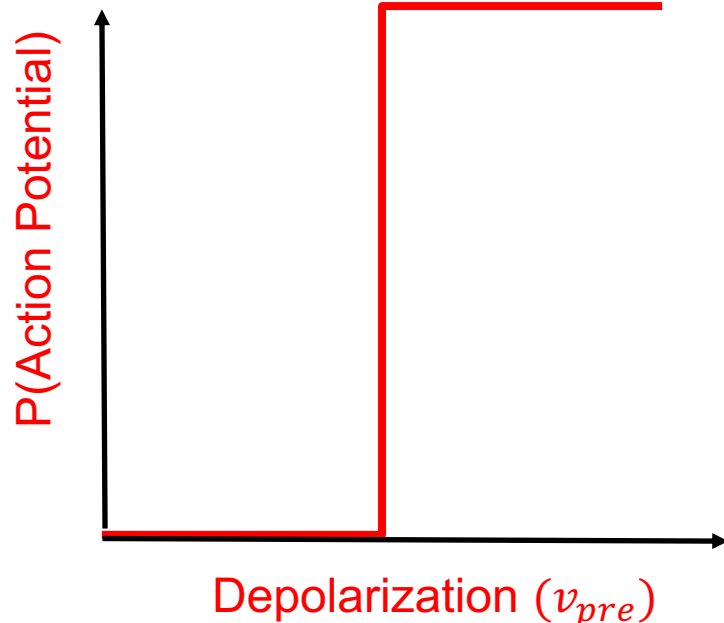
Spiny stellate cells



Pyramidal cells

$$v_{post} = \sigma(v_{pre}) \otimes h$$

$H(v_{pre})$ Heaviside function



Take a population of spiny stellate cells & assume either:

1. Unimodal distribution over firing thresholds
2. Unimodal distribution over population Membrane depolarizations

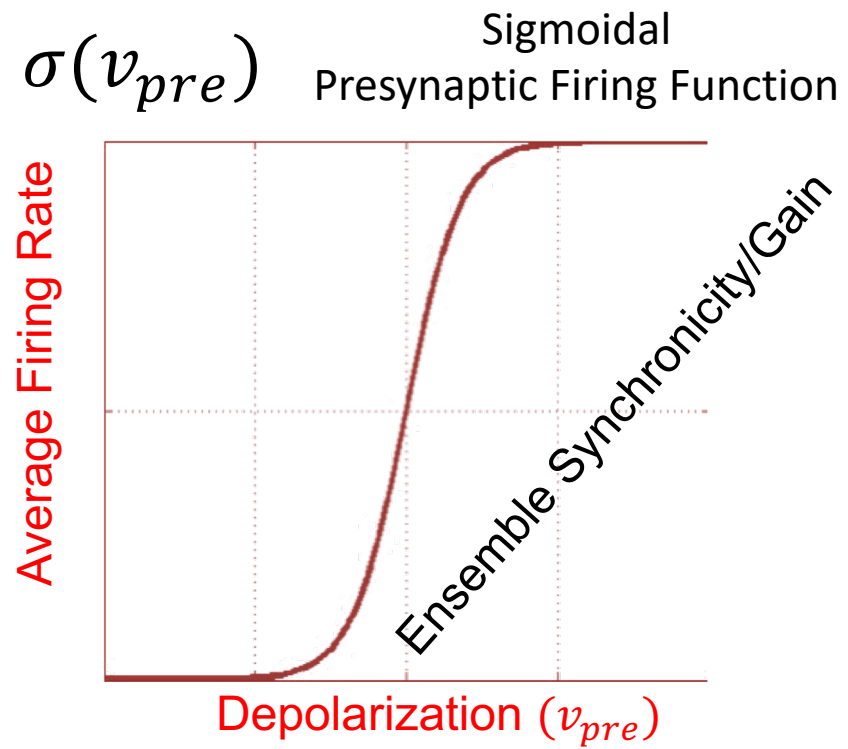
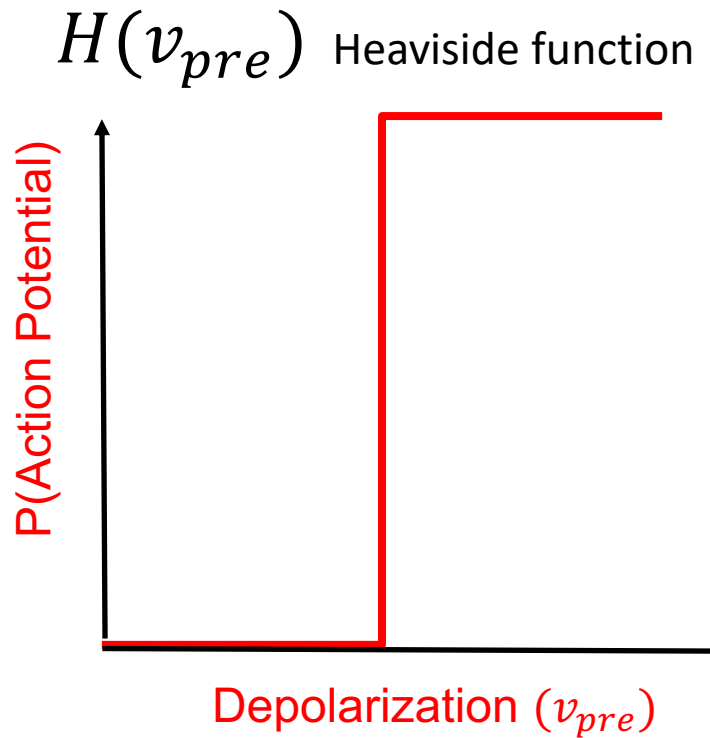
Convolution-Based Neural Mass Models in DCM

Spiny stellate cells



Pyramidal cells

$$v_{post} = \sigma(v_{pre}) \otimes h$$



Convolution-Based Neural Mass Models in DCM

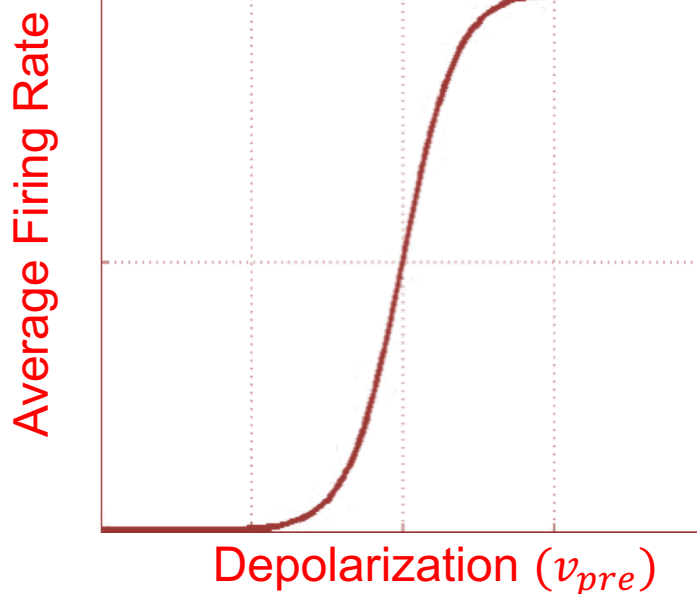
Spiny stellate cells



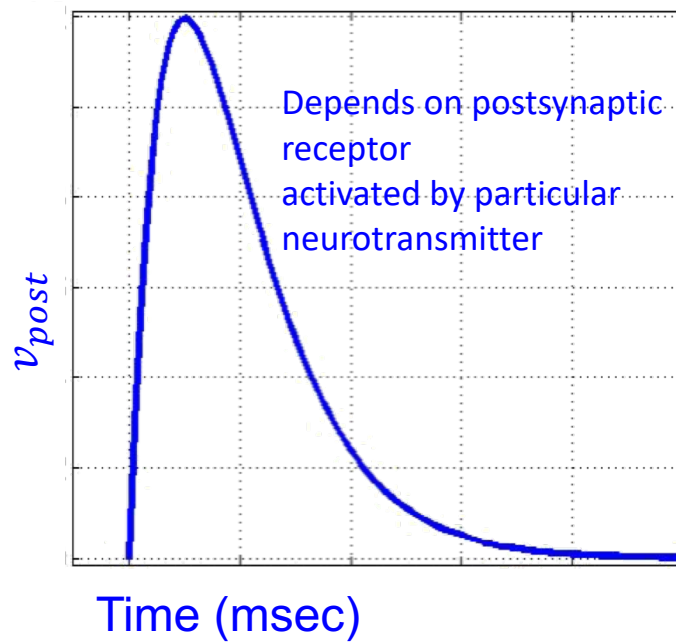
Pyramidal cells

$$v_{post} = \sigma(v_{pre}) \otimes h$$

$\sigma(v_{pre})$ Sigmoidal Presynaptic Firing Function



h Postsynaptic Kernel



Convolution-Based Neural Mass Models in DCM

Spiny stellate cells

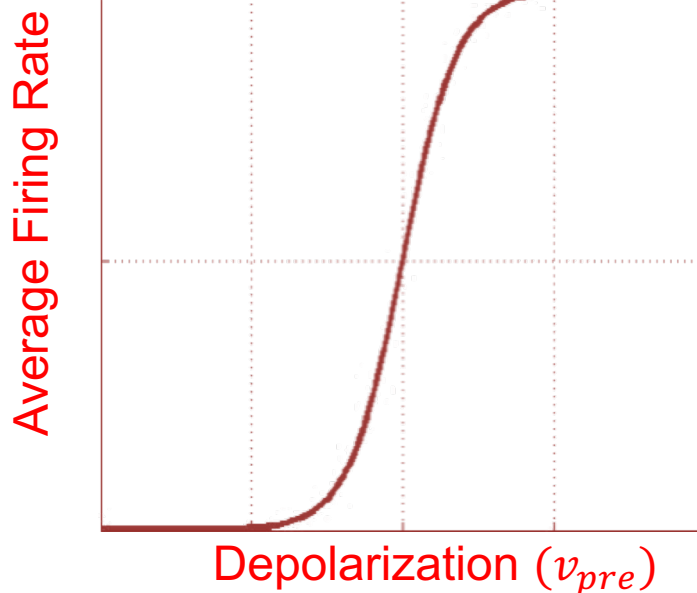


Pyramidal cells

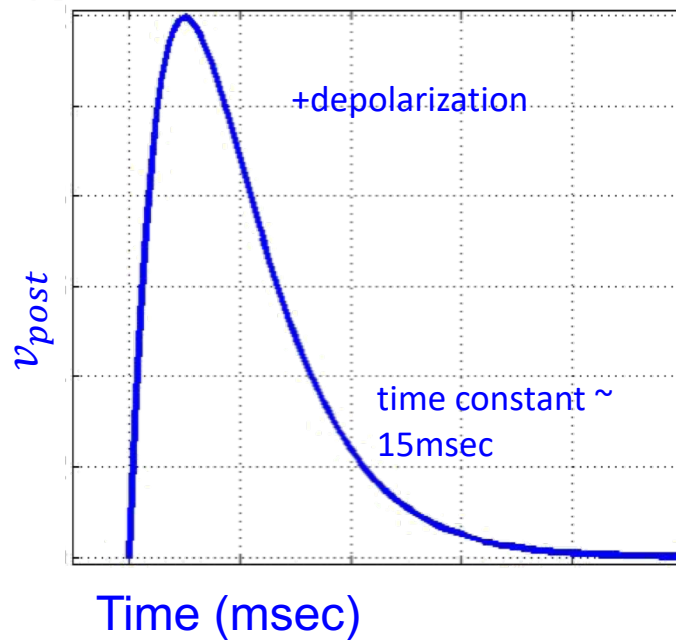
E.g. Glutamate from SS to AMPA receptor

$$v_{post} = \sigma(v_{pre}) \otimes h$$

$\sigma(v_{pre})$ Sigmoidal Presynaptic Firing Function

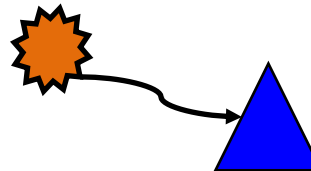


h Postsynaptic Kernel



Convolution-Based Neural Mass Models in DCM

Inhibitory interneuron

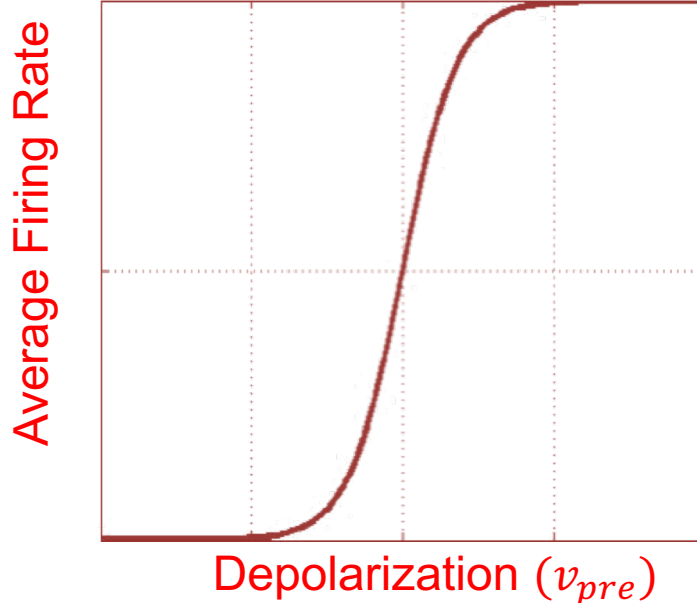


E.g. GABA from inhibitory interneuron to GABA_A receptor

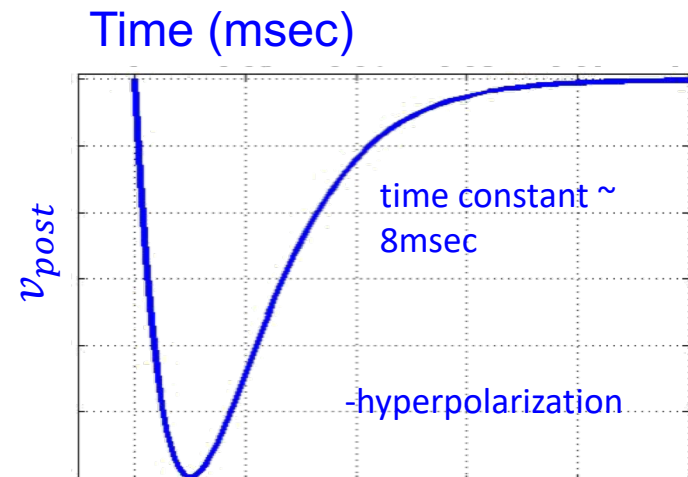
Pyramidal cells

$$v_{post} = \sigma(v_{pre}) \otimes h$$

$\sigma(v_{pre})$ Sigmoidal Presynaptic Firing Function



h Postsynaptic Kernel



Convolution-Based Neural Mass Models in DCM

Spiny stellate cells



γ

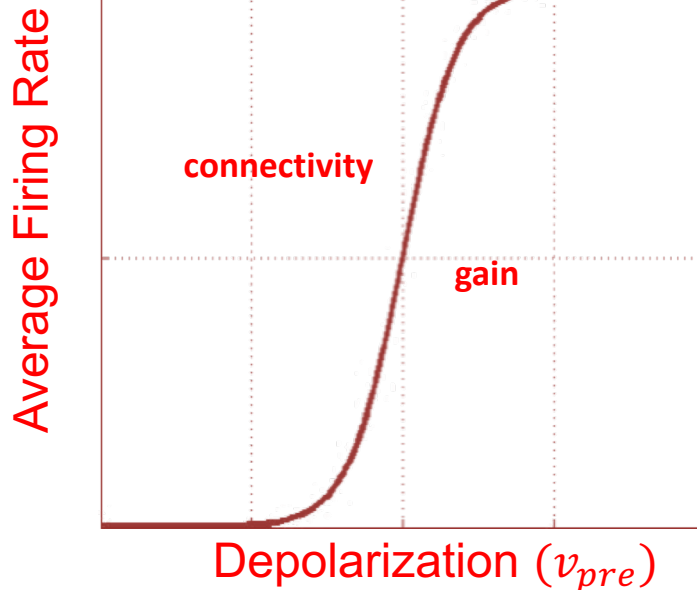
Pyramidal cells

Connectivity?

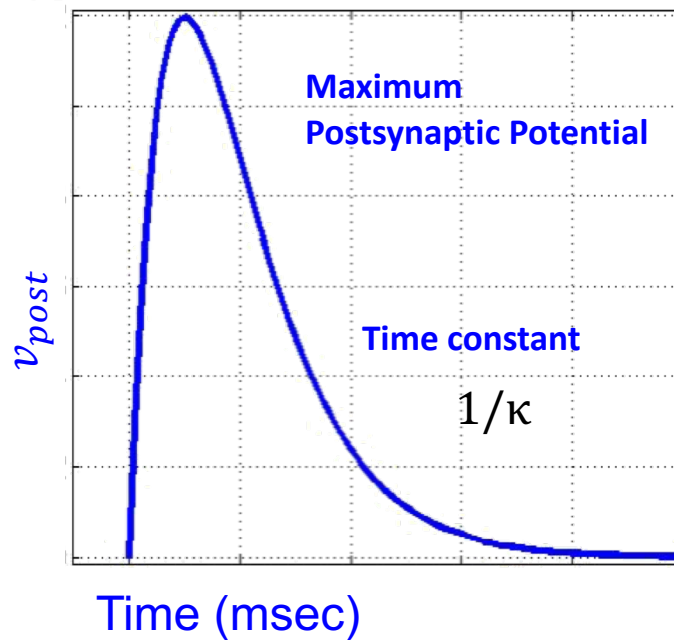
$$v_{post} = \gamma \sigma(v_{pre}) \otimes h$$

$$\theta = \{\gamma, gain, H, \tau\}$$

$\gamma \sigma(v_{pre})$ Sigmoidal Presynaptic Firing Function



h Postsynaptic Kernel



Convolution to ODEs

Spiny stellate cells



Pyramidal cells

$$v_{post} = \gamma \sigma(v_{pre}) \otimes h$$

$$v_{post} = \int_0^t h(t - \tau) \gamma \sigma(v_{pre}) d\tau$$

Convolution Equation

$$\ddot{v_{post}} = H\kappa\gamma\sigma(v_{pre}) - 2\kappa\dot{v_{post}} - \kappa v_{post}$$

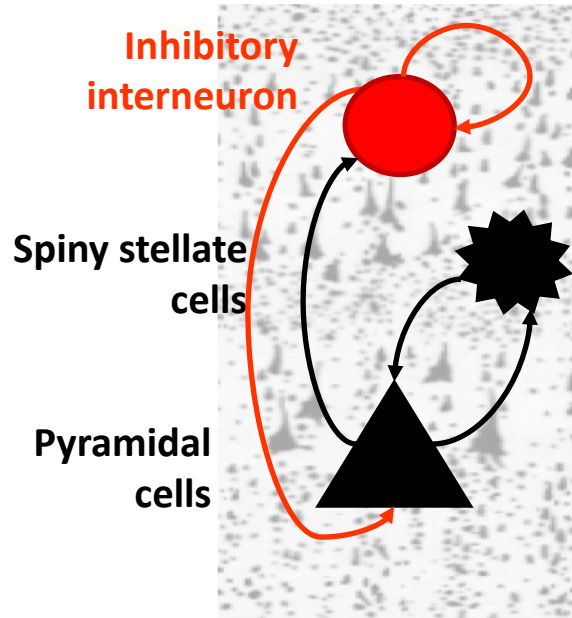
By parts twice

Second Order Differential Equation

$$\begin{aligned}\dot{v_{post}} &= i \\ \dot{i} &= H\kappa\gamma\sigma(v_{pre}) - 2\kappa i - \kappa v_{post}\end{aligned}$$

2 Coupled First Order Differential
For each transmitter receptor pair

Multilaminar NMMS



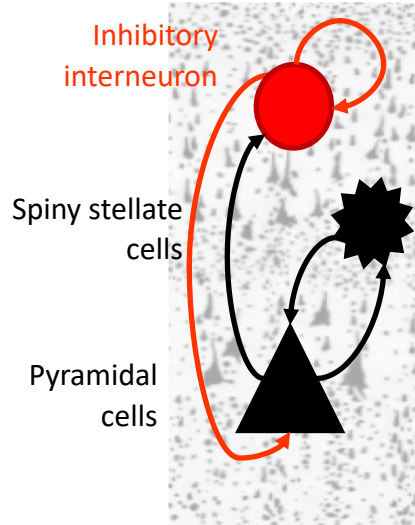
Assume GABA from inhibitory interneurons activate GABAa receptors

Assume glutamate from pyramidal cells & spiny stellate cells activate AMPA receptors

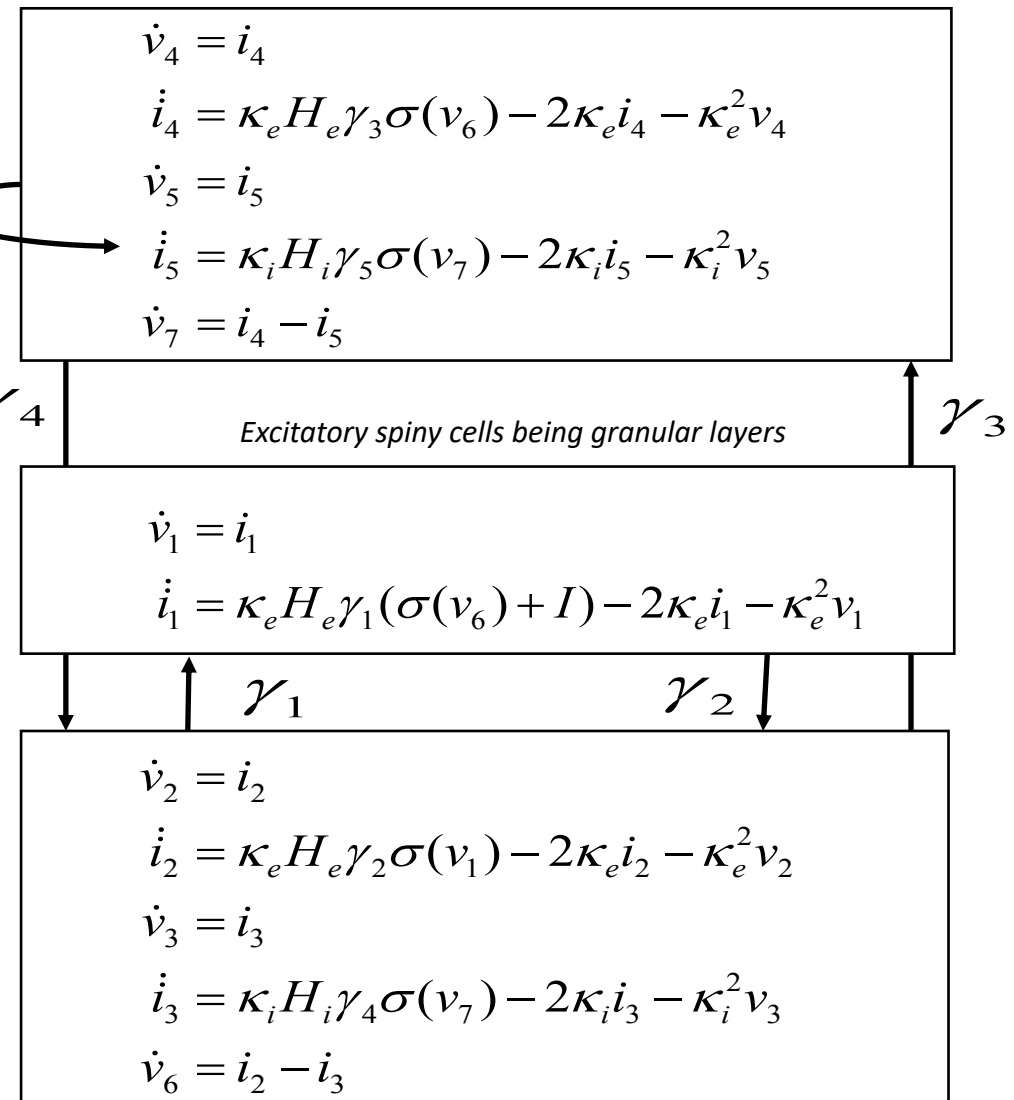
Then construct interlaminar connectivity

5 connections giving 5×2 coupled first order differential equations

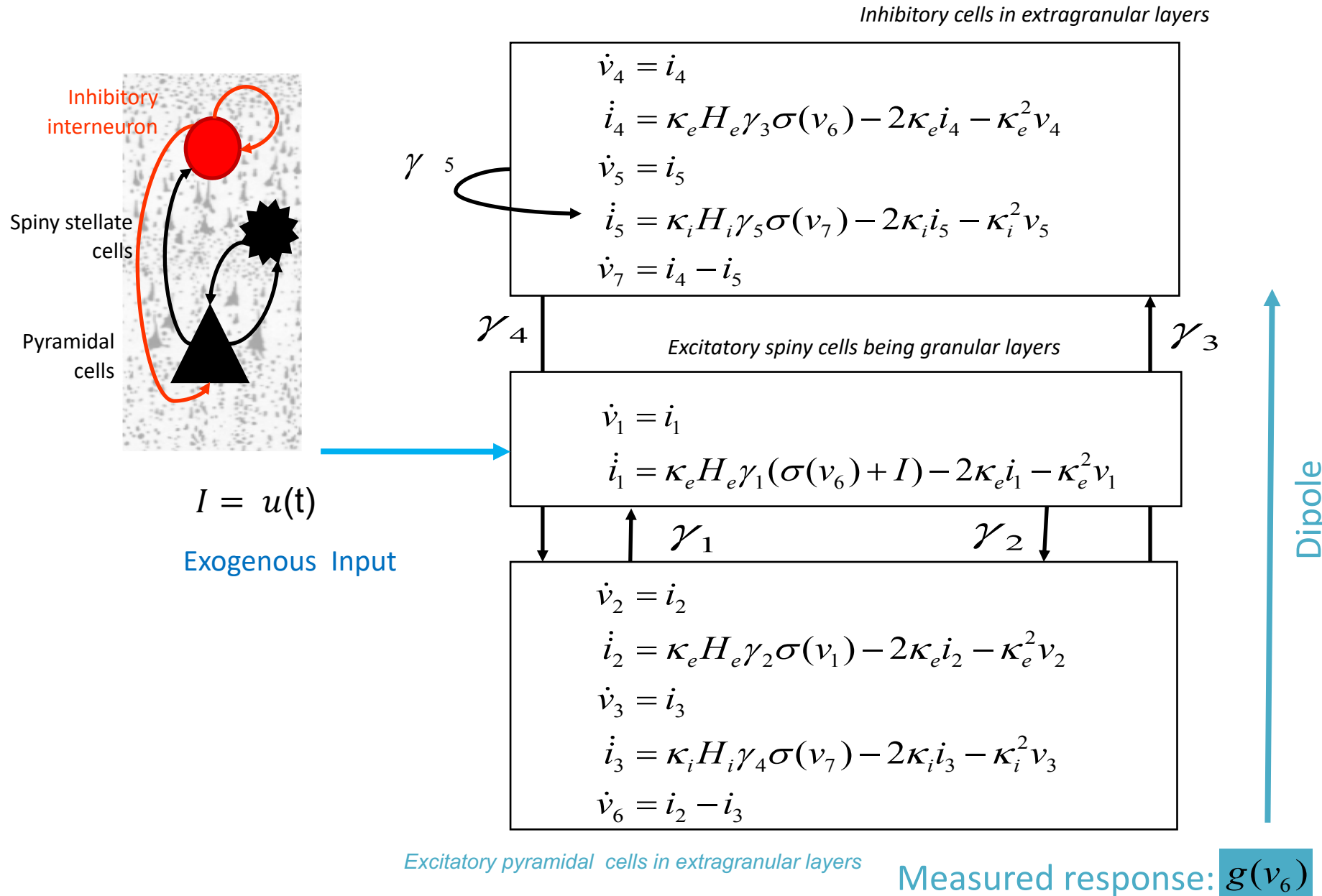
One region: 12 equations 10 + 2 difference



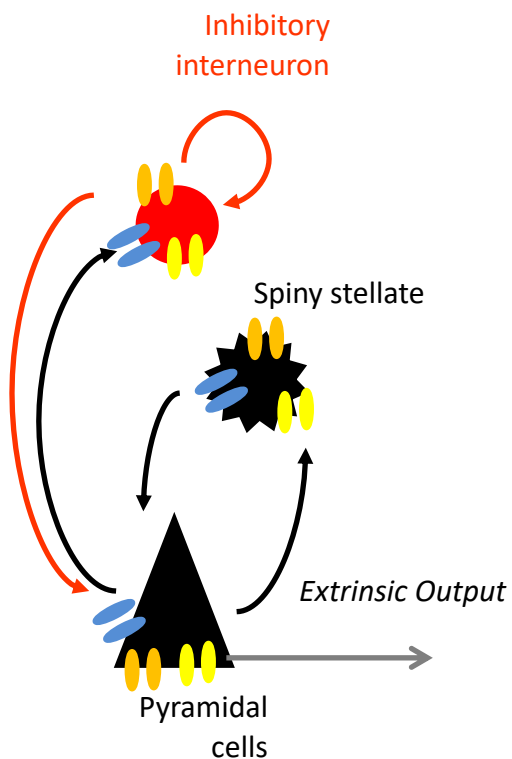
Inhibitory cells in extragranular layers



One region: 12 equations 10 + 2 difference

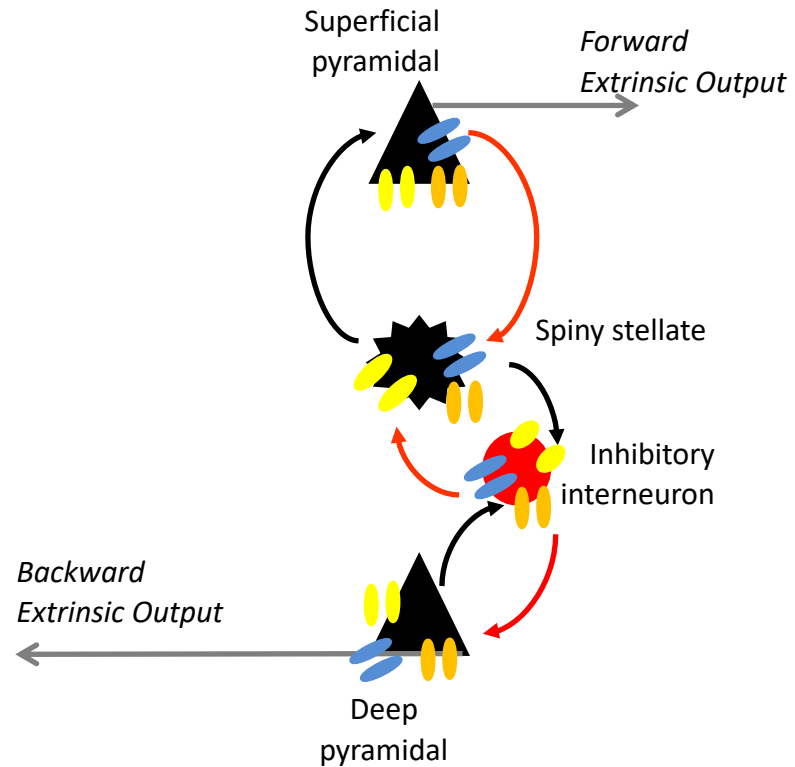


Predictive coding-based Neural Mass Models in DCM



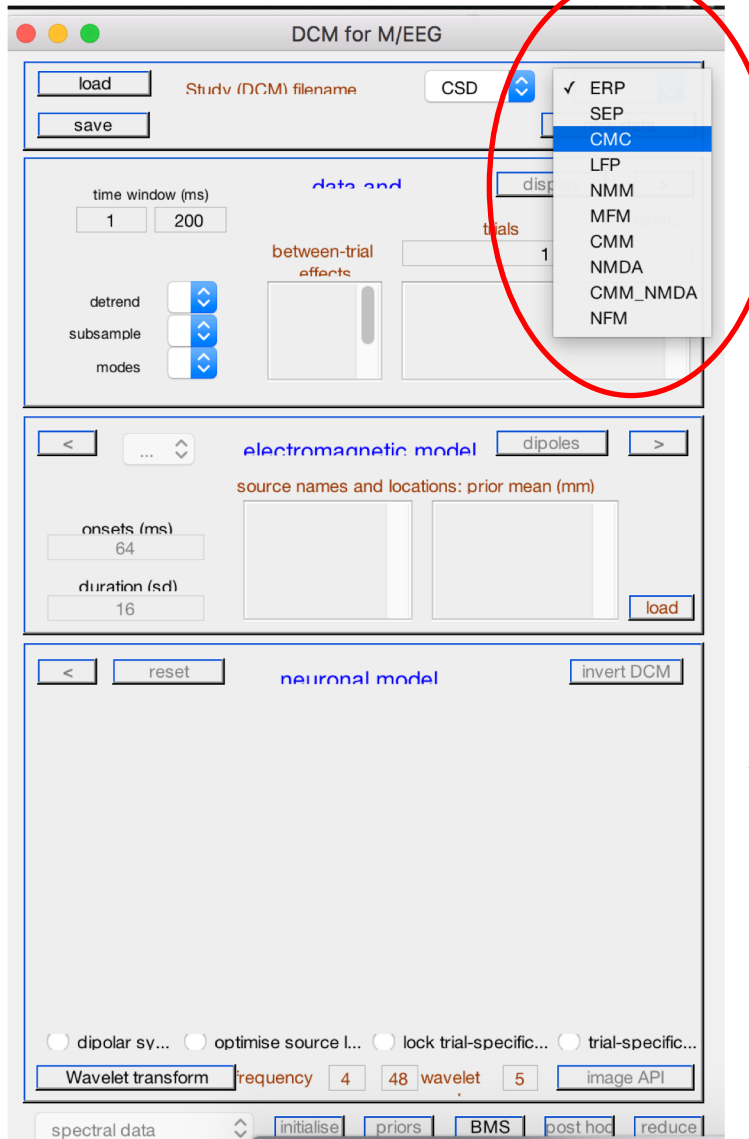
Canonical Microcircuits for Predictive Coding

Andre M. Bastos,^{1,2,6} W. Martin Usrey,^{1,3,4} Rick A. Adams,⁵ George R. Mangun,^{2,3,5} Pascal Fries,^{6,7} and Karl J. Friston^{8,*}



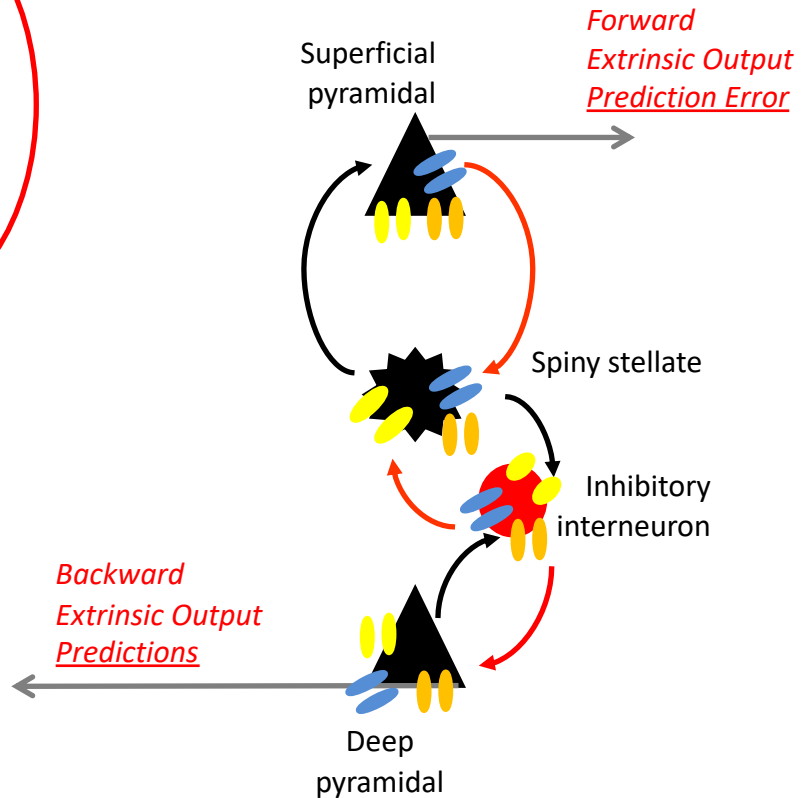
**4-subpopulation
Canonical Microcircuit**

Predictive coding-based Neural Mass Models in DCM



Canonical Microcircuits for Predictive Coding

Andre M. Bastos,^{1,2,6} W. Martin Usrey,^{1,3,4} Rick A. Adams,⁵ George R. Mangun,^{2,3,5} Pascal Fries,^{6,7} and Karl J. Friston^{8,*}



4-subpopulation
Canonical Microcircuit

Conductance Based Neural Mass Models

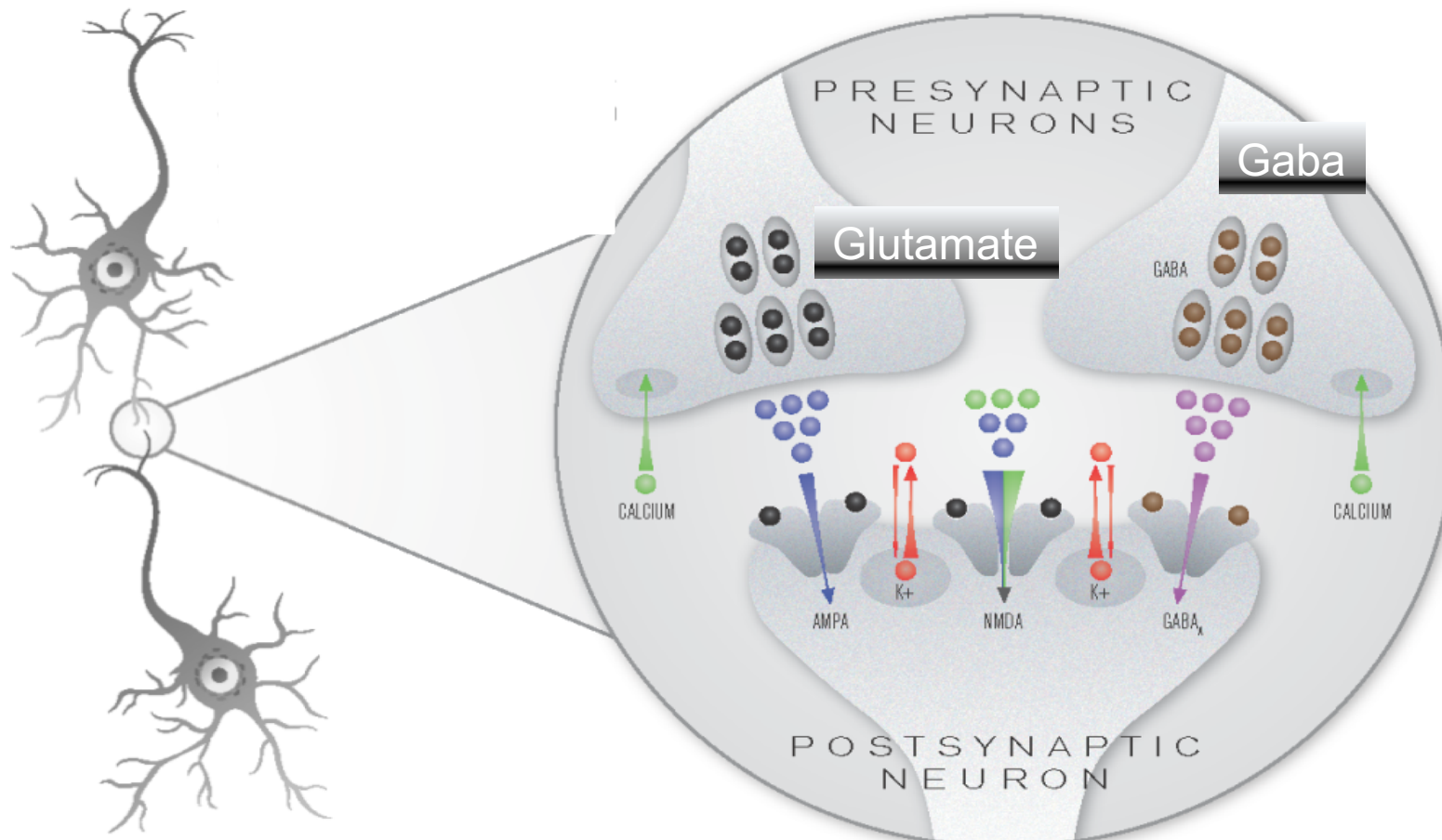
Conductance-Based Neural Mass Models in DCM

Current in = Conductance X Potential Difference

$$C\dot{V} = g(V_{rev} - V)$$

Ohm's Law $V = IR$

Ohm's Law for a Capacitor $I = C \frac{dv}{dt}$



Conductance-Based Neural Mass Models in DCM

Current in = Conductance X Potential Difference

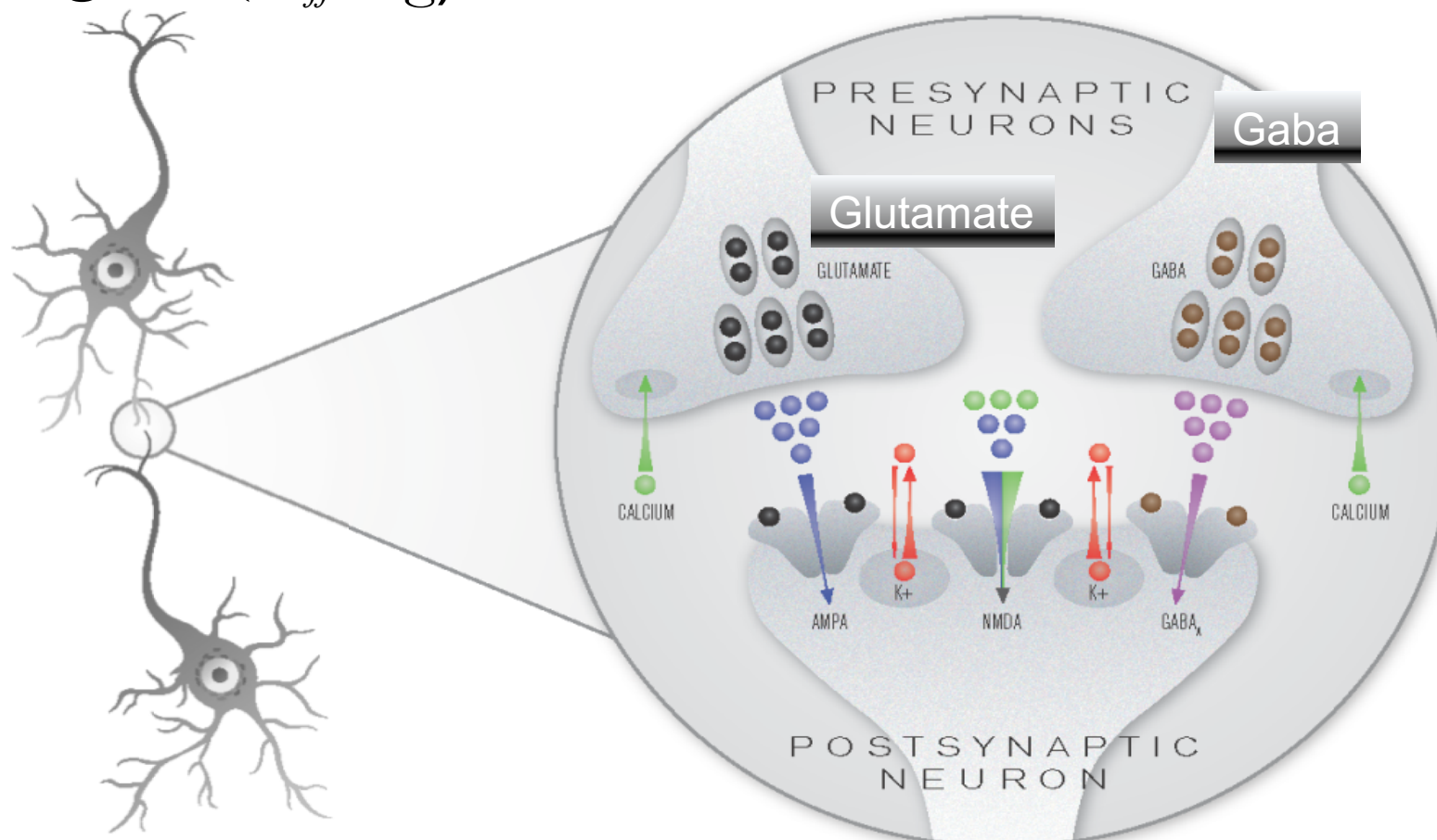
$$C\dot{V} = g(V_{rev} - V)$$

$$\dot{g} = \kappa(\gamma_{aff} - g)$$

Ohm's Law $V = IR$

Ohm's Law for a Capacitor $I = C dv/dt$

Dynamic Conductance



Conductance-Based Neural Mass Models in DCM

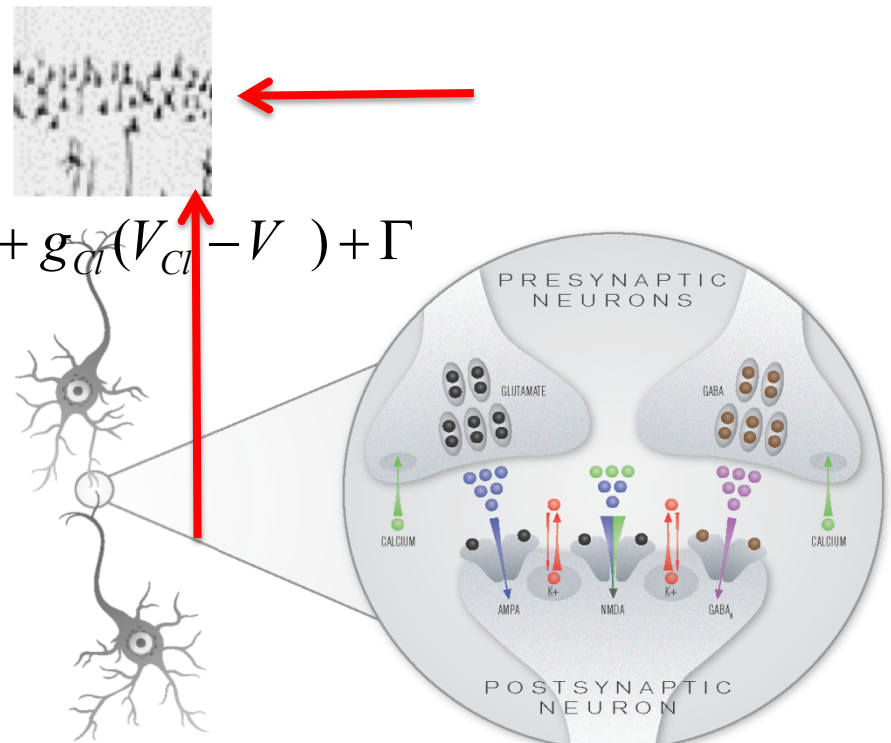
Connectivity driven by different neurotransmitters and receptors

$$\dot{CV} = g_{Na}(V_{Na} - V) + g_{Ca}f_{MG}(V_{Ca} - V) + g_{Cl}(V_{Cl} - V) + \Gamma$$

$$\dot{g}_{Na} = \kappa_{AMPA}(\gamma_{ec}\sigma - g_{Na}) + \Gamma$$

$$\dot{g}_{Cl} = \kappa_{GABA}(\gamma_{it}\sigma - g_{Cl}) + \Gamma$$

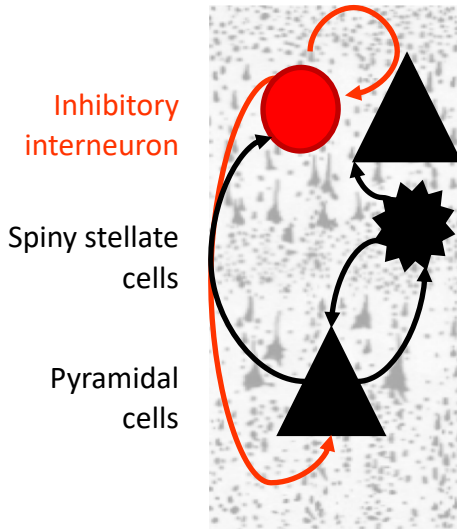
$$\dot{g}_{Ca} = \kappa_{NMDA}(\gamma_{ec}\sigma - g_{Ca}) + \Gamma$$



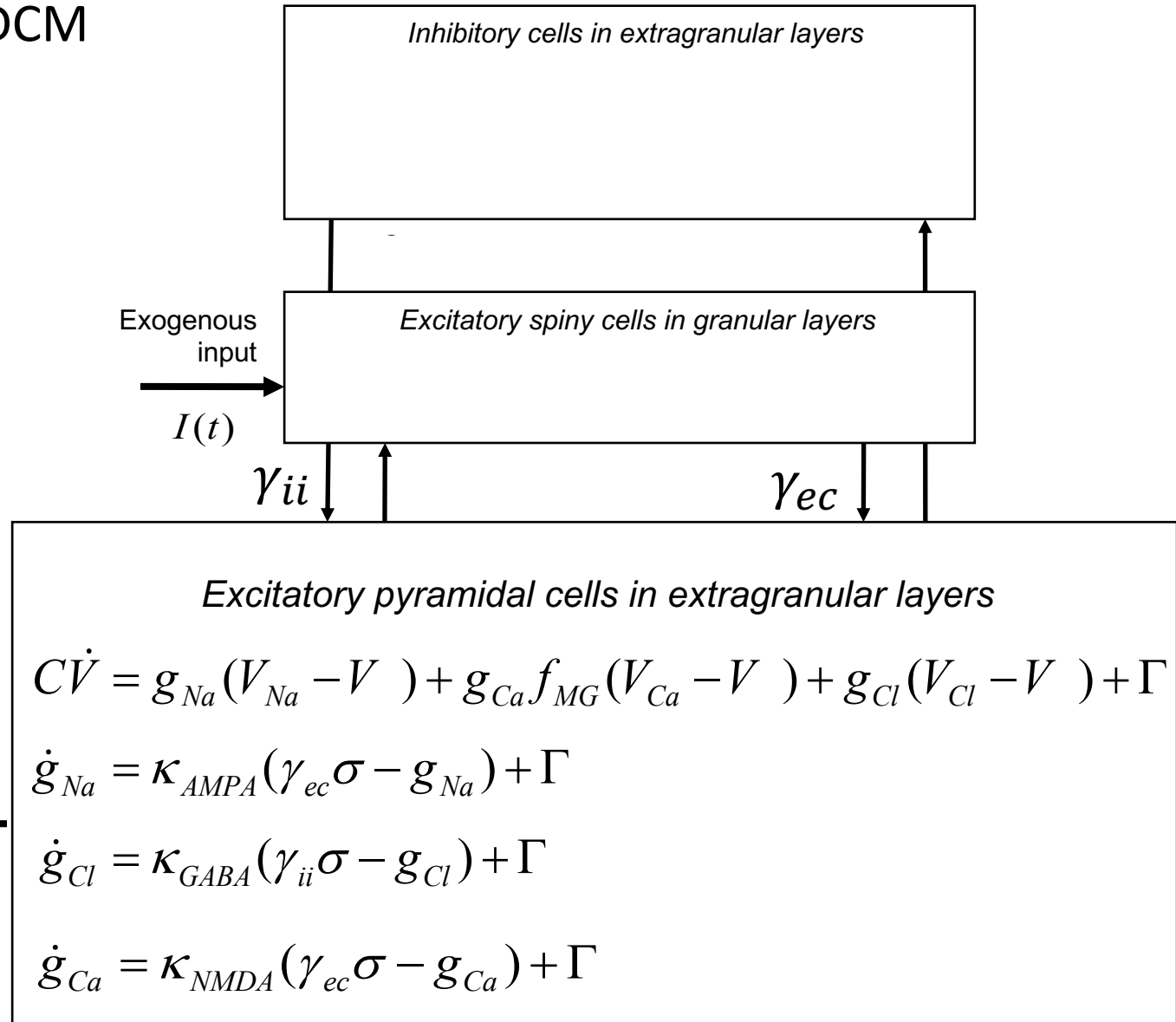
State equations & parameters

$$\dot{x} = F(x, u, \theta) \quad \theta = \{\gamma, \kappa, V_{rev}, V_{thresh}, C\}$$

Conductance-Based Neural Mass Models in DCM



Inhibitory interneuron
Spiny stellate cells
Pyramidal cells



A selection of intrinsic architectures in SPM (e.g. conductance based CMC)

frontiers in
COMPUTATIONAL NEUROSCIENCE

REVIEW ARTICLE
published: 28 May 2013
doi: 10.3389/fncom.2013.00057



Neural masses and fields in dynamic causal modeling

Rosalyn Moran^{1,2,3*}, Dimitris A. Pinotsis^{1†} and Karl Friston¹

¹ Wellcome Trust Centre for Neuroimaging, Institute of Neurology, University College London, London, UK

² Virginia Tech Carilion Research Institute, Virginia Tech, Roanoke, VA, USA

³ Bradley Department of Electrical and Computer Engineering, Virginia Tech, Blacksburg, VA, USA

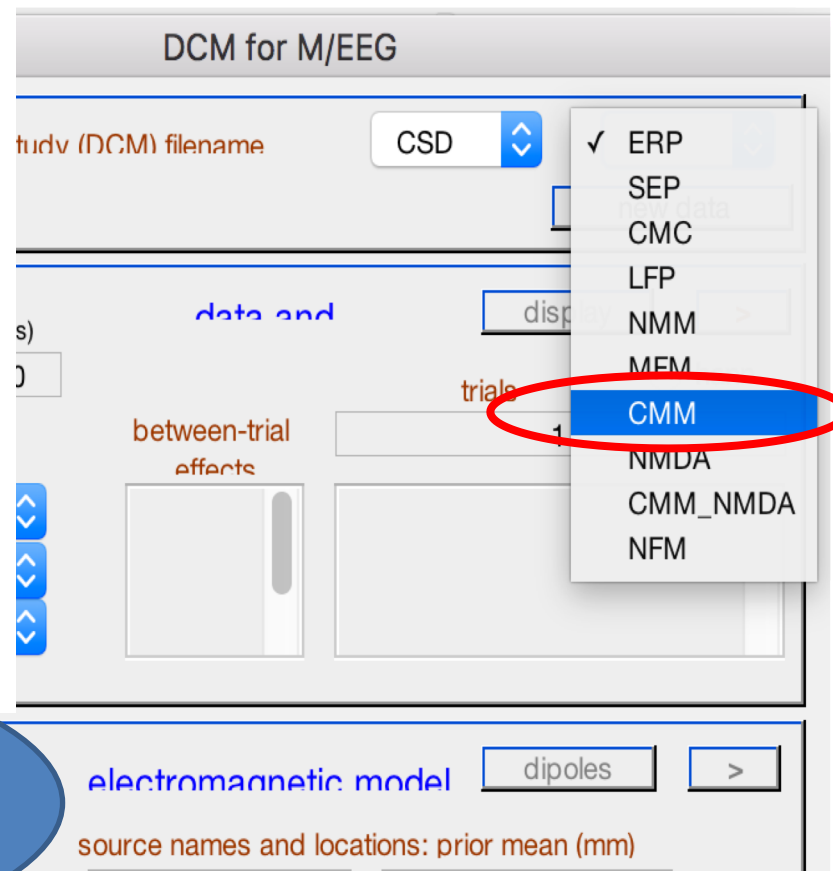
Edited by:
Peter Robinson, University of
Sydney, Australia

Reviewed by:
Peter Robinson, University of
Sydney, Australia
James Roberts, Queensland
Institute of Medical Research,
Australia

***Correspondence:**
Rosalyn Moran, Virginia Tech Carilion
Research Institute, Virginia Tech,
2 Riverside Drive, Roanoke,
24016 VA, USA
e-mail: rosalyn@vtc.vt.edu
[†]These authors have contributed
equally to this work.

Dynamic causal modeling (DCM) provides a framework for the analysis of effective connectivity among neuronal subpopulations that subtend invasive (electrocorticograms and local field potentials) and non-invasive (electroencephalography and magnetoencephalography) electrophysiological responses. This paper reviews the suite of neuronal population models including neural masses, fields and conductance-based models that are used in DCM. These models are expressed in terms of sets of differential equations that allow one to model the synaptic underpinnings of connectivity. We describe early developments using neural mass models, where convolution-based dynamics are used to generate responses in laminar-specific populations of excitatory and inhibitory cells. We show that these models, though resting on only two simple transforms, can recapitulate the characteristics of both evoked and spectral responses observed empirically. Using an identical neuronal architecture, we show that a set of conductance based models—that consider the dynamics of specific ion-channels—present a richer space of responses; owing to non-linear interactions between conductances and membrane potentials. We propose that conductance-based models may be more appropriate when spectra present with multiple resonances. Finally, we outline a third class of models, where each neuronal subpopulation is treated as a field; in other words, as a manifold on the cortical surface. By explicitly accounting for the spatial propagation of cortical activity through partial differential equations (PDEs), we show that the topology of connectivity—through local lateral interactions among cortical layers—may be inferred, even in the absence of spatially resolved data. We also show that these models allow for a detailed analysis of structure-function relationships in the cortex. Our review highlights the relationship among these models and how the appropriate model class.

A suite of neuronal population models
including neural masses, fields and
conductance-based models...expressed in
terms of sets of differential equations



Forward Model: Neural Mass Models in DCM

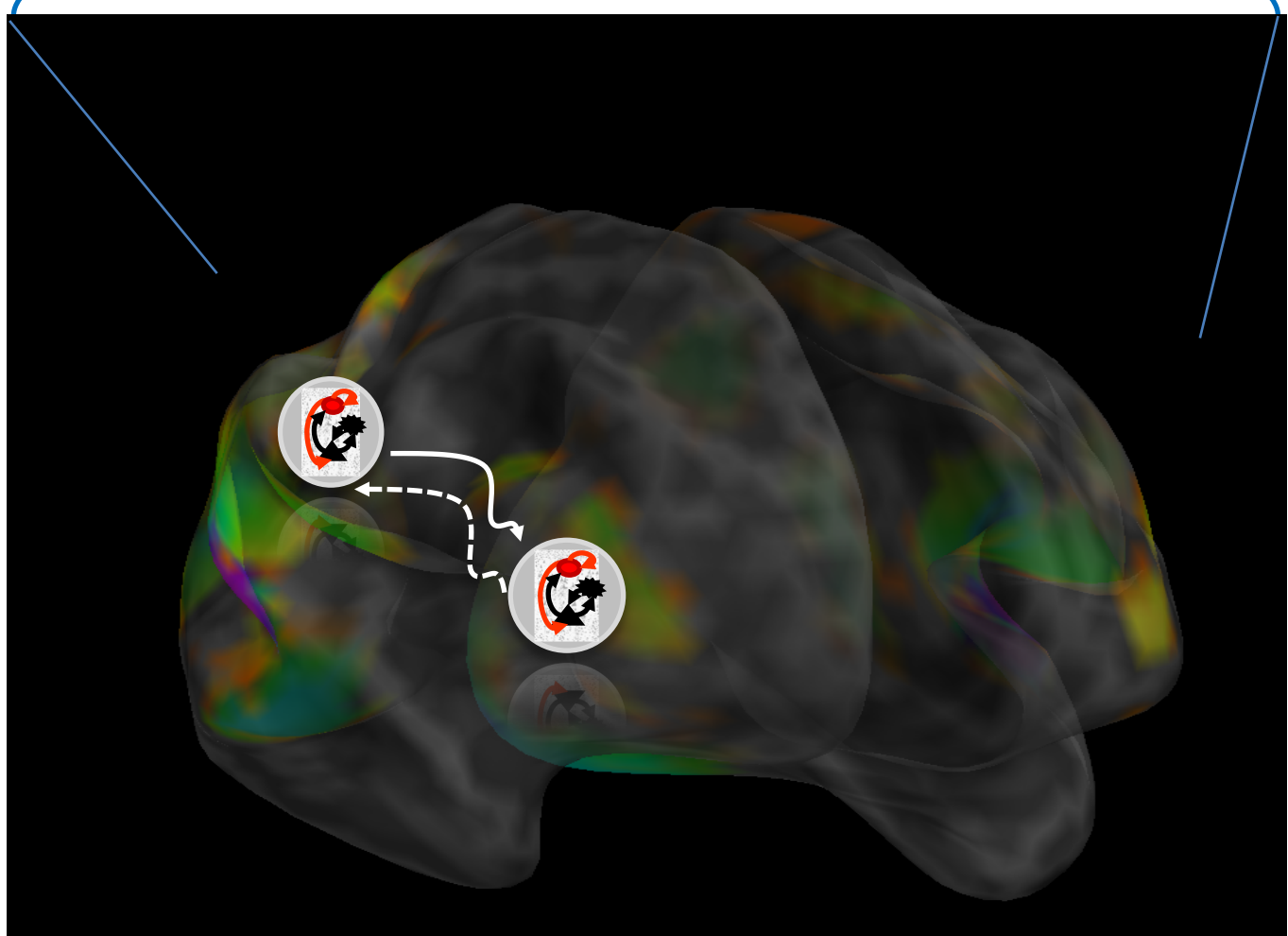
Empirical
Observations
(eg Sensor Level)

$$Y = g(\theta_g, v_6)$$

Lead Field

$$\dot{v} = f(\theta_f, u)$$

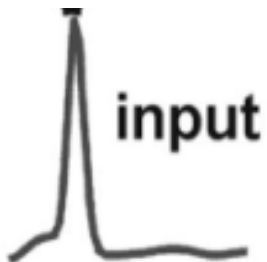
Interconnected
Neural mass
models



Neural Mass Models in DCM for ERPs

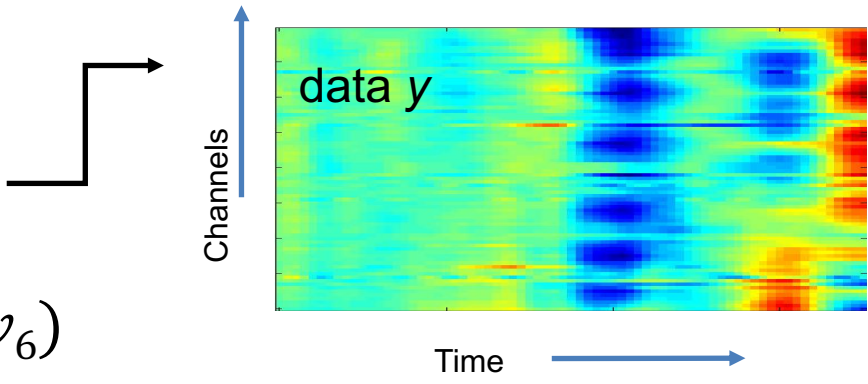
$$u = u(t) \quad \xrightarrow{\text{ }} \quad Y = g(\theta_g, v_6)$$

Lead Field



$$\dot{v} = f(\theta_f, u)$$

Interconnected
Neural mass
models



Event-Related
Potentials

State equations from time to spectral domain

Time Differential Equations

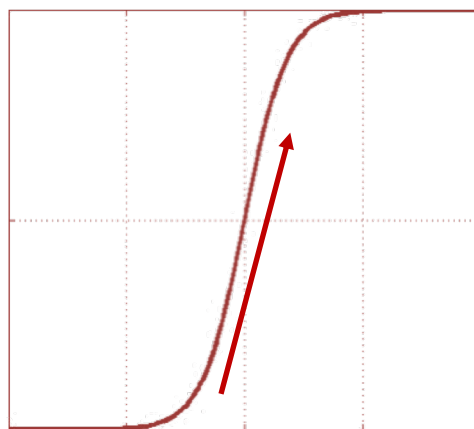
$$Y = g(\theta_g, v_6)$$
$$\dot{v} = f(\theta_f, u)$$

mV

White/Pink Noise

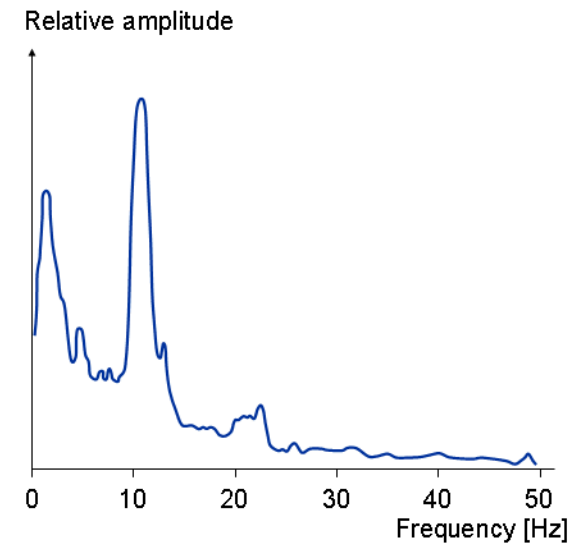
Linearise

$$Y = g(\theta_g, v_6)$$
$$\dot{v} = A(\theta_f) + Bu$$



Analytic Transfer
Function in the
Frequency domain

$$H(s) = g(sI - A)B$$

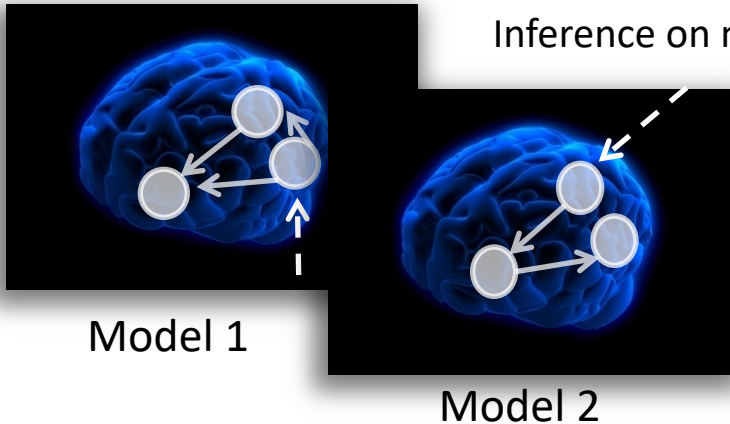


Model Inversion & Inference

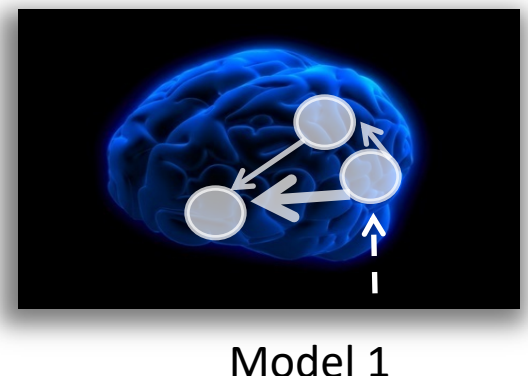
Bayes' rules: $p(\theta | y, m) = \frac{p(y | \theta, m)p(\theta | m)}{p(y | m)}$

Free Energy: $F_{\max} = \ln p(y|m) - D(q(\theta) \| p(\theta|y,m))$

Bayesian Inversion



Inference on parameters

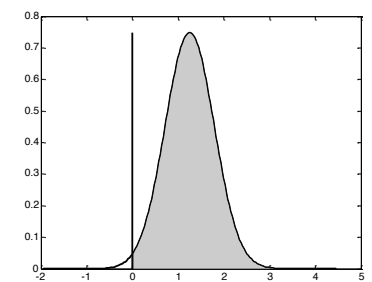


Model comparison via Bayes factor:

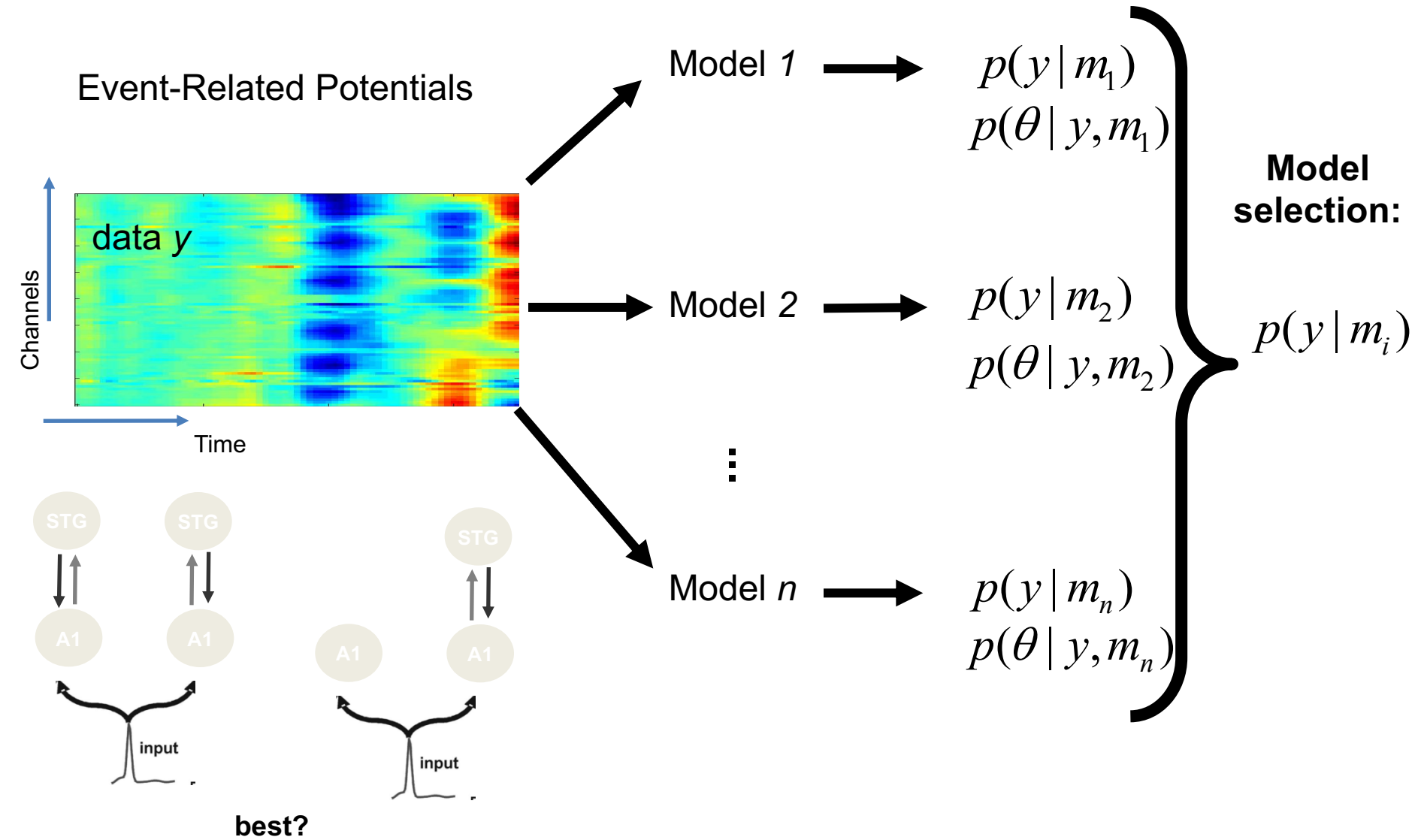
$$BF = \frac{p(y | m_1)}{p(y | m_2)}$$

→ accounts for both accuracy and complexity of the model

→ allows for inference about structure (generalisability) of the model

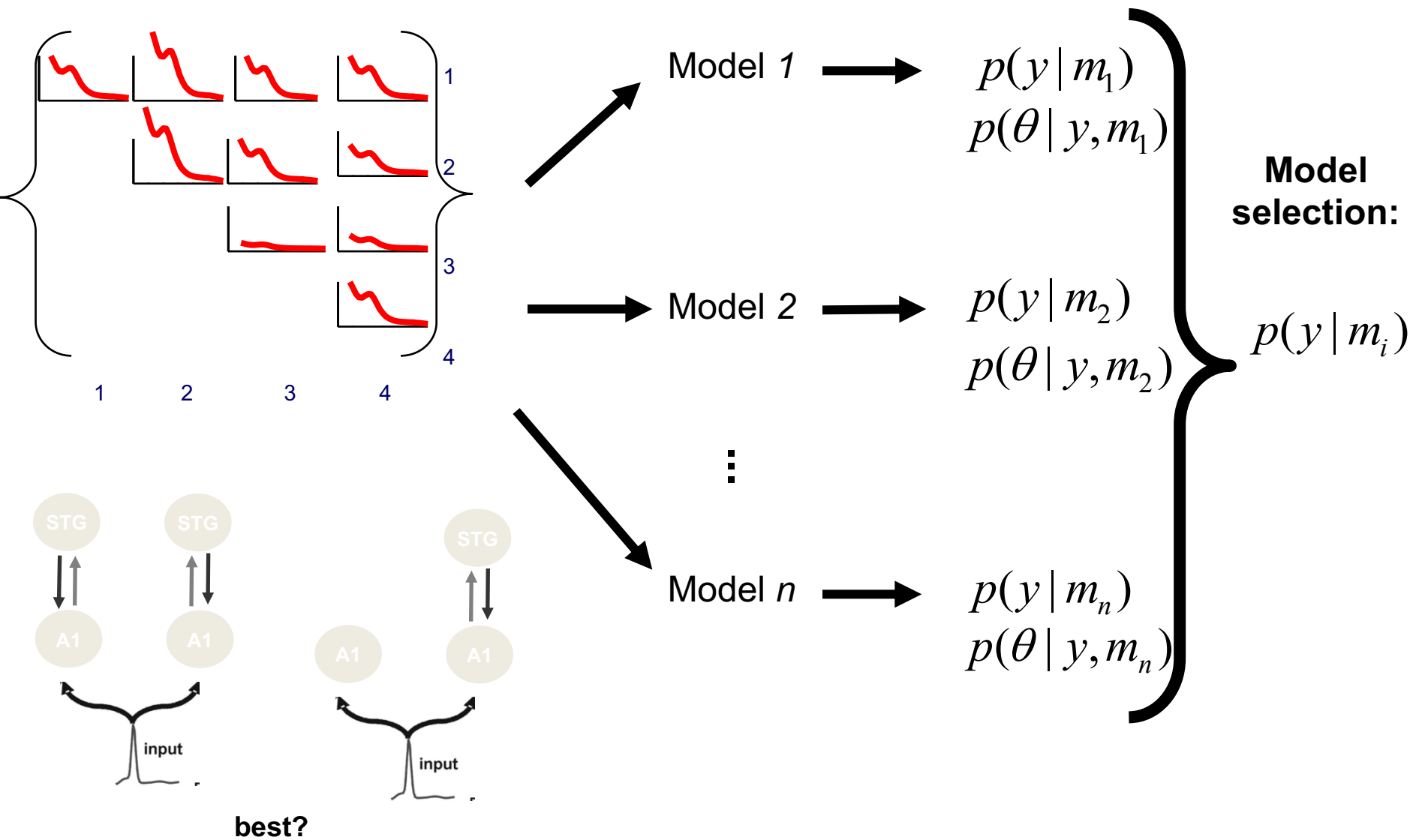


Data & Hypotheses



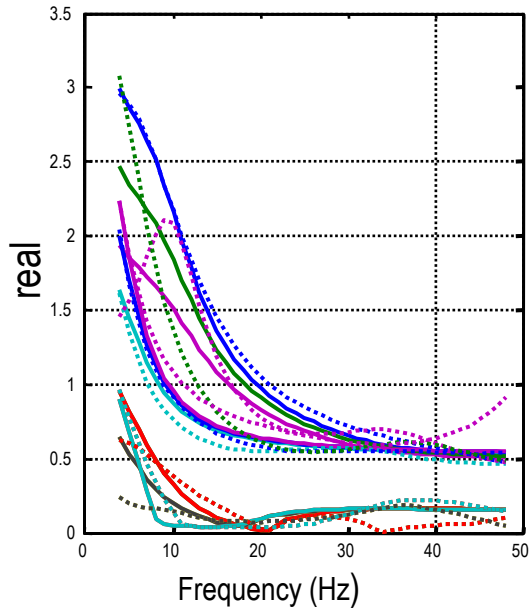
Data & Hypotheses

Cross-Spectral Responses

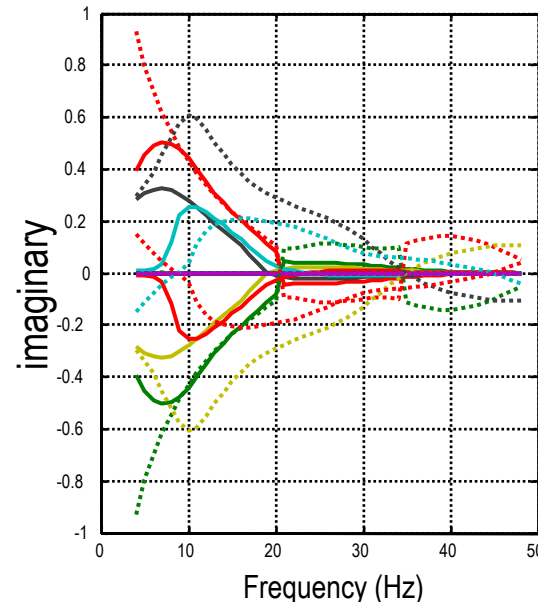


Inversion in the real & complex domain

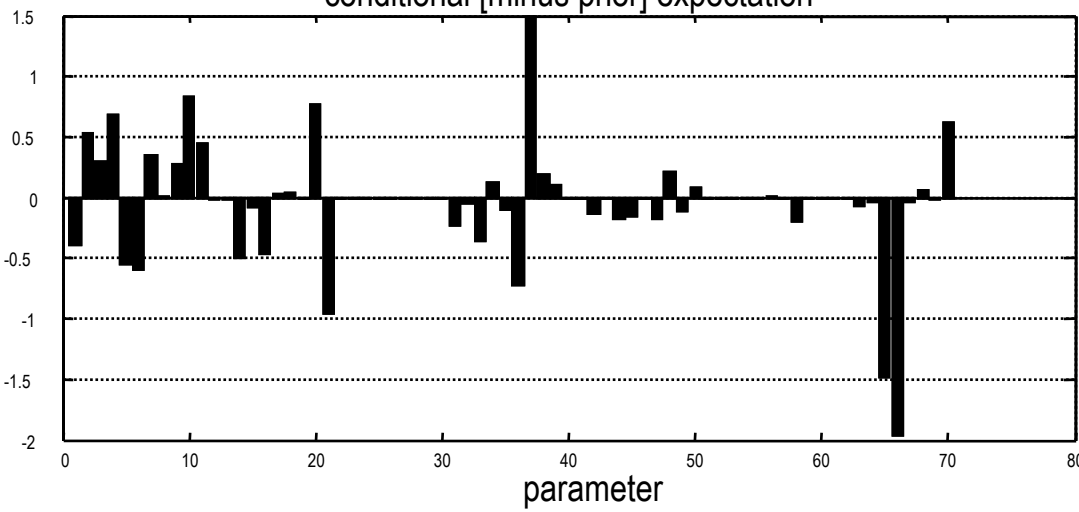
prediction and response: E-Step: 32



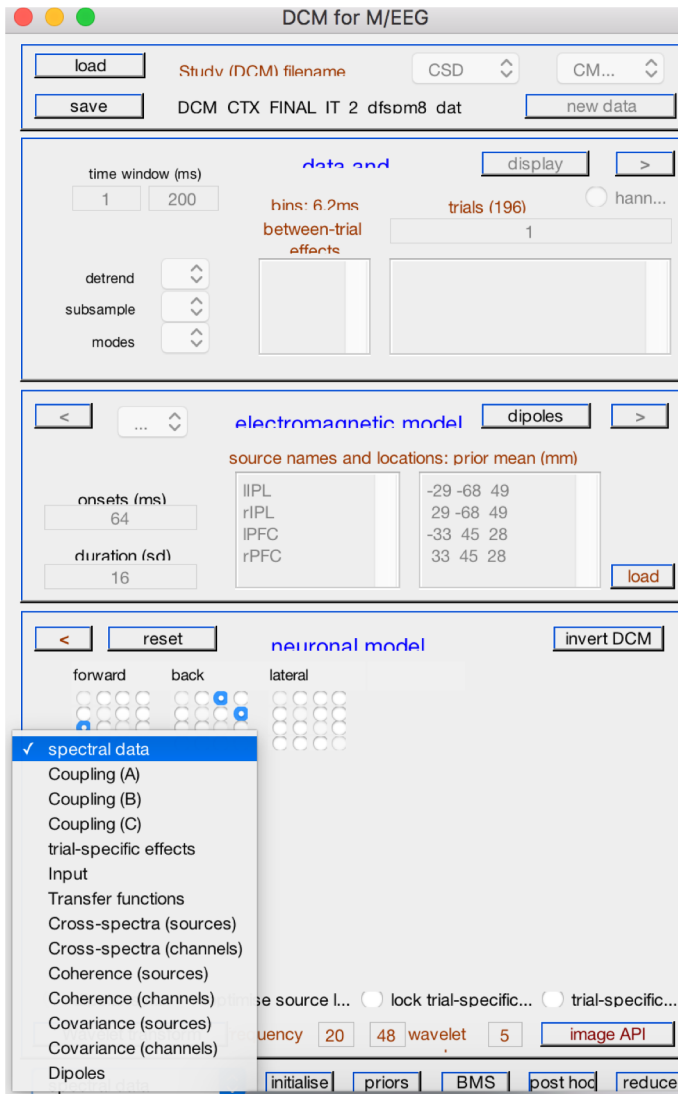
prediction and response: E-Step: 32



conditional [minus prior] expectation



Coherence for free!



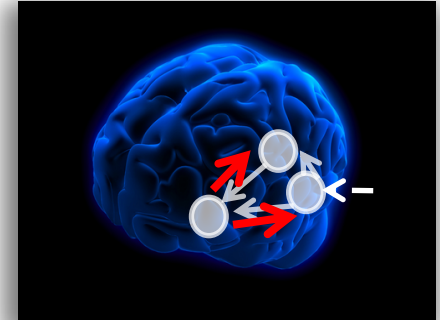
(derivatives of the data features
also recapitulated in the models)

$$Coh_{12} = \frac{|CSD_1 CSD_2^*|}{CSD_1 CSD_2}$$

**(Complex Conjugate)*

DCM for EEG Examples

Connectivity changes underlying spectral EEG changes during propofol-induced loss of consciousness.



Wake

Mild Sedation: Responsive to command

Deep Sedation: Loss of Consciousness



Propofol-induced loss of consciousness

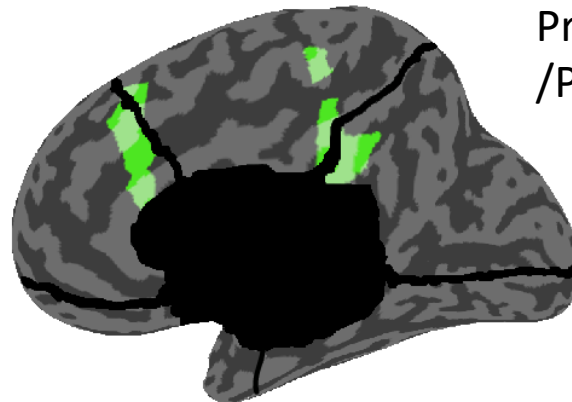
Wake

Mild Sedation: Responsive to command

Deep Sedation: Loss of Consciousness



Anterior
Cingulate
/mPFC



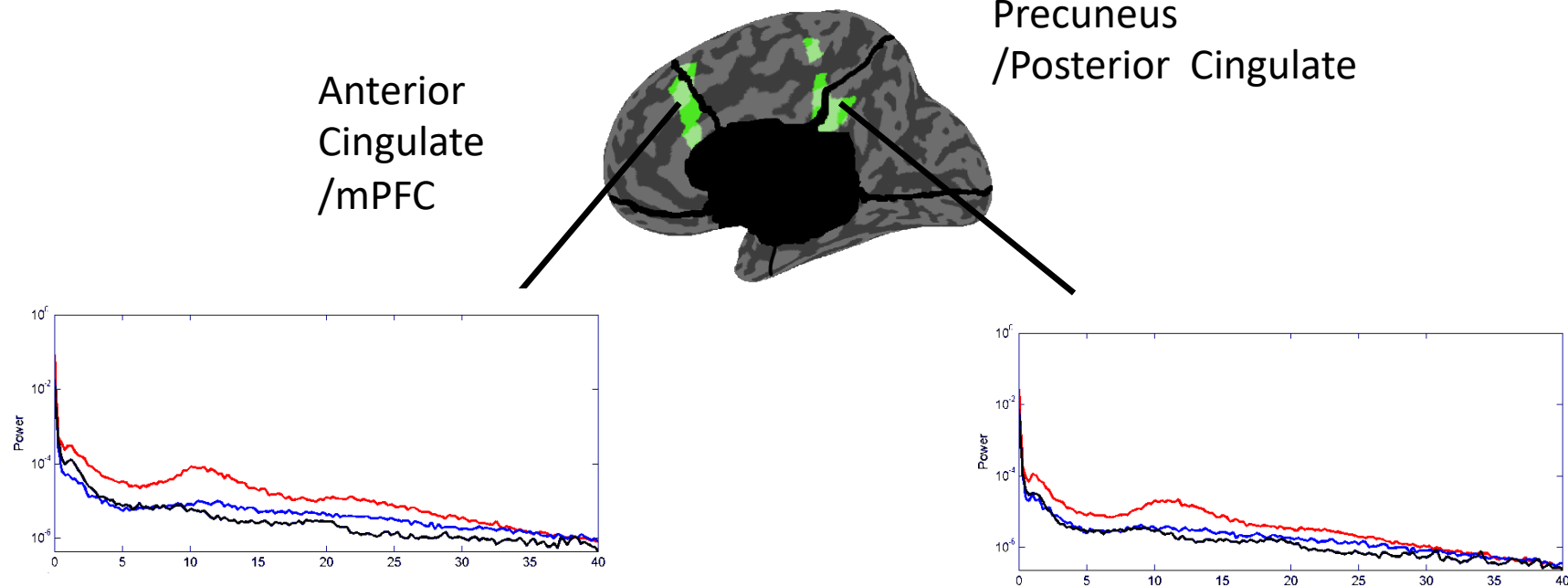
Precuneus
/Posterior Cingulate

Propofol-induced loss of consciousness

Wake

Mild Sedation: Responsive to command

Deep Sedation: Loss of Consciousness

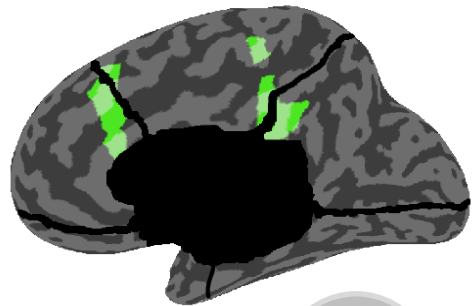


Murphy et al. 2011

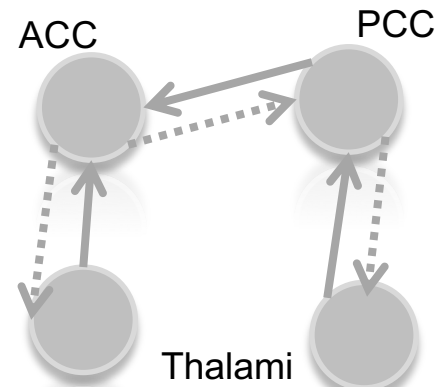
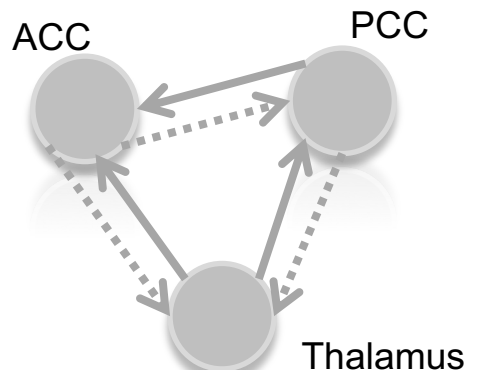
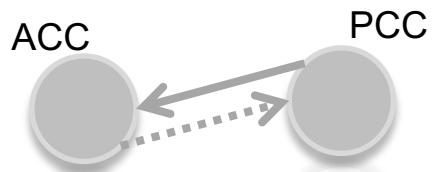
*Increased gamma power in Propofol vs Wake
Increased low frequency power when consciousness is lost*

Propofol-induced loss of consciousness

Wake
Mild Sedation
Deep Sedation



Bayesian Model Selection

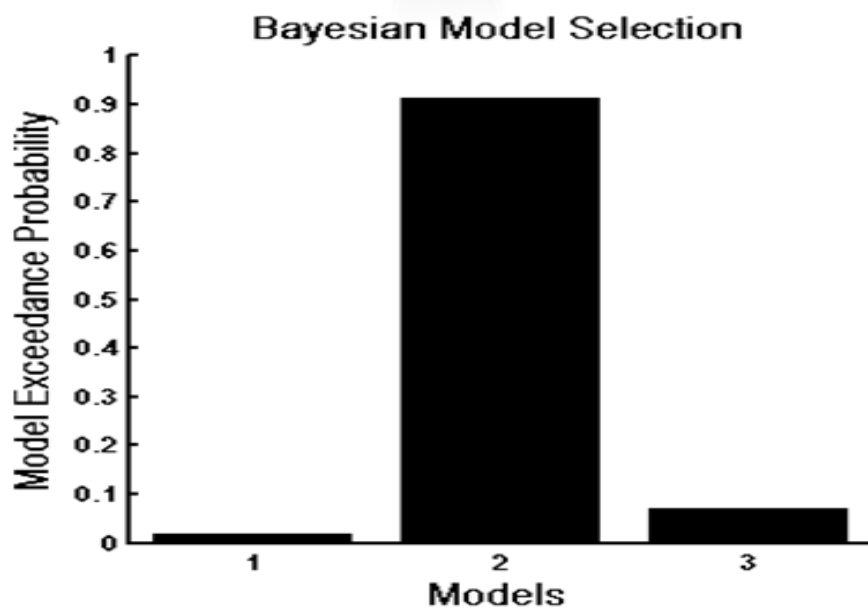
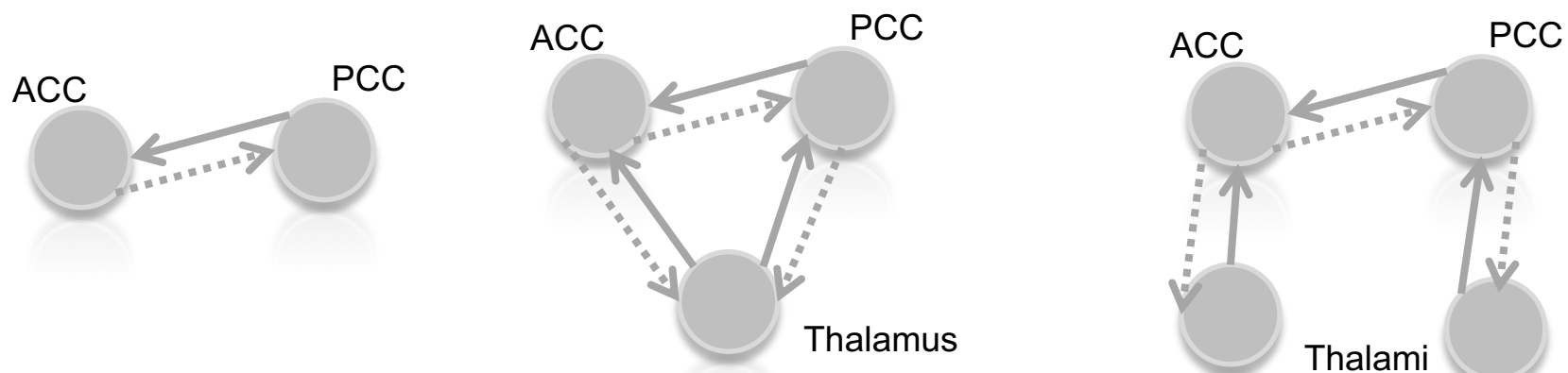
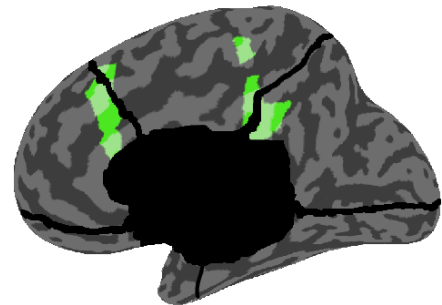


Propofol-induced loss of consciousness

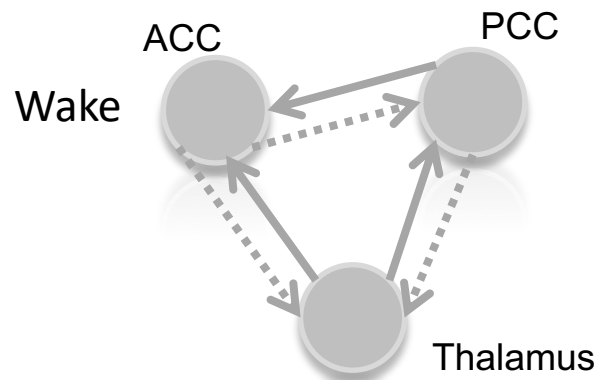
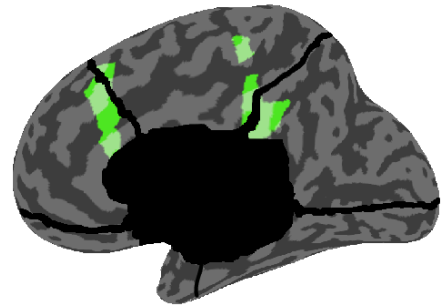
Wake

Mild Sedation

Deep Sedation

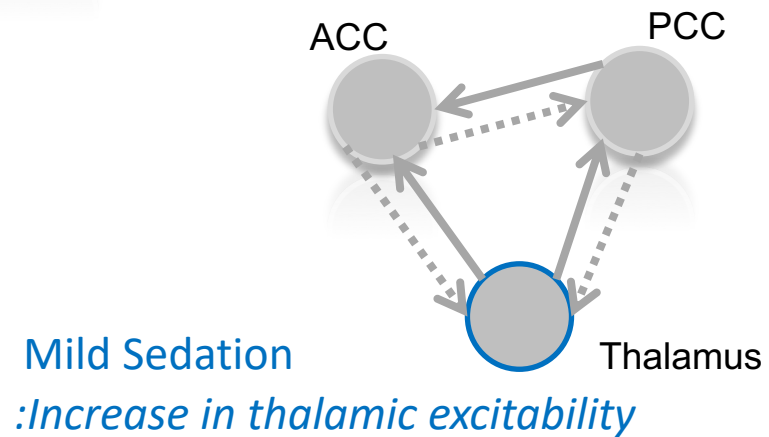
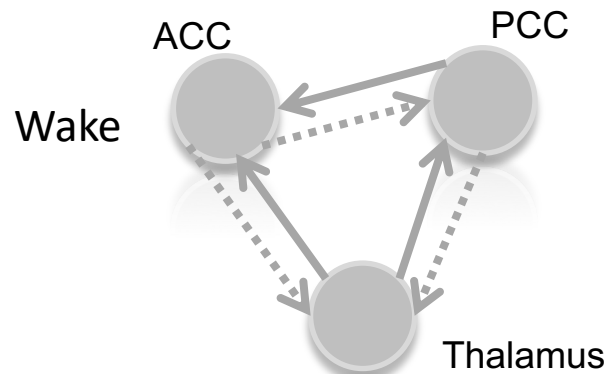
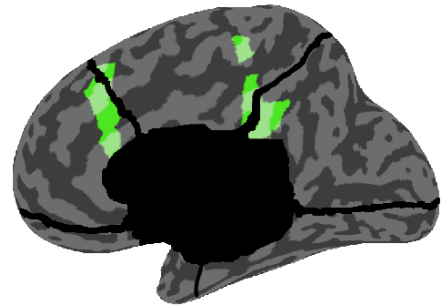


Propofol-induced loss of consciousness

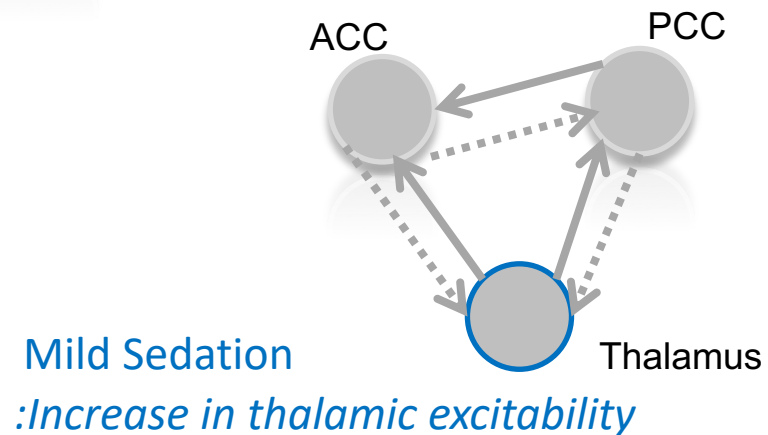
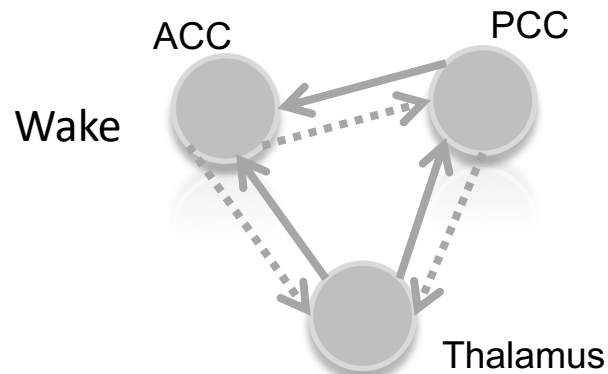


Parameters of Winning Model

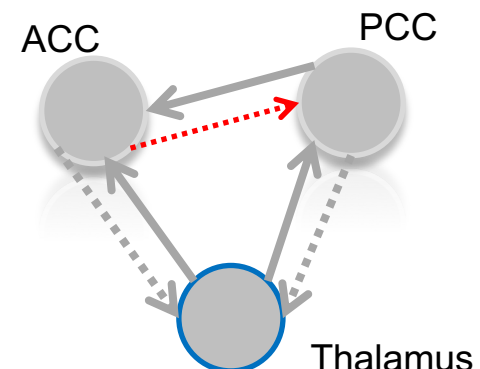
Propofol-induced loss of consciousness



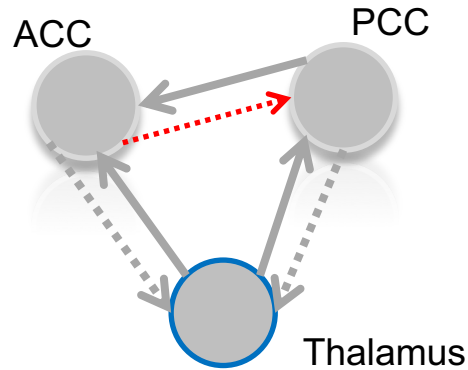
Propofol-induced loss of consciousness



Loss of Consciousness
:Breakdown in Cortical Backward Connections



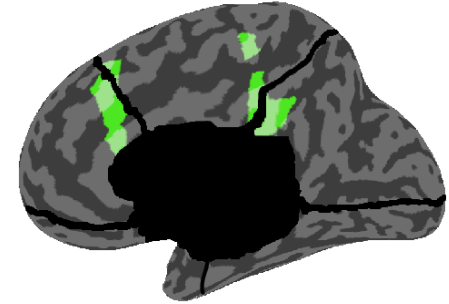
Propofol-induced loss of consciousness



Loss of Consciousness

:Breakdown in Cortical Backward Connections

Boly, Moran, Murphy,
Boveroux, Bruno, Noirhomme,
Ledoux, Bonhomme, Brichant,
Tononi, Laureys, Friston, J Neuroscience, 2012



Preserved Feedforward But Impaired Top-Down Processes in the Vegetative State
Melanie Boly, et al.
Science 332, 858 (2011);
DOI: 10.1126/science.1202043

Preserved Feedforward But Impaired Top-Down Processes in the Vegetative State

Melanie Boly,^{1,2*} Marta Isabel Garrido,² Olivia Gosseries,¹ Marie-Aurélie Bruno,¹ Pierre Boveroux,³ Caroline Schnakers,¹ Marcello Massimini,⁴ Vladimir Litvak,² Steven Laureys,¹ Karl Friston²

Frontoparietal cortex is involved in the explicit processing (awareness) of stimuli. Frontoparietal activation has also been found in studies of subliminal stimulus processing. We hypothesized that an impairment of top-down processes, involved in recurrent neuronal message-passing and the generation of long-latency electrophysiological responses, might provide a more reliable correlate of consciousness in severely brain-damaged patients, than frontoparietal responses. We measured effective connectivity during a mismatch negativity paradigm and found that the only significant difference between patients in a vegetative state and controls was an impairment of backward connectivity from frontal to temporal cortices. This result emphasizes the importance of top-down projections in recurrent processing that involve high-order associative cortices for conscious perception.

The vegetative state (VS) is defined by preserved arousal, in the absence of any behavioral signs of awareness (*1*). In contrast,

patients in a minimally conscious state (MCS) show nonreflexive and purposeful behaviors but are unable to communicate (*2*). Because the clin-

ical diagnosis of these patients is extremely difficult (*3*), neuroimaging experiments have tried to establish accurate biomarkers of consciousness level in VS and MCS. These patients also provide a lesion-deficit model in the quest for neural correlates of consciousness in the human brain (*4*). The conscious perception of external stimuli requires activation of frontoparietal cortices, in addition to activity in low-level specialized cortices (*5–7*). However, frontoparietal activation can also be found during subliminal stimulus processing (*8, 9*). Current evidence points to long-latency evoked event-related potential (ERP) components, involving frontoparietal cortices, as a reliable neu-

¹Coma Science Group, Cyclotron Research Centre and Neurology Department, University of Liège and CHU Sart Tilman Hospital, 4000 Liège, Belgium. ²Wellcome Trust Centre for Neuroimaging, Institute of Neurology, University College London, London WC1N 1PF, UK. ³Anesthesiology Department, University of Liège and CHU Sart Tilman Hospital, 4000 Liège, Belgium. ⁴Department of Clinical Sciences, “Luigi Sacco,” University of Milan, 20137 Milan, Italy.

*To whom correspondence should be addressed. E-mail: mboly@ulg.ac.be

The Ketamine Model of Psychosis & Schizophrenia

Noncompetitive NMDA-r antagonist

Dissociative anaesthetic:

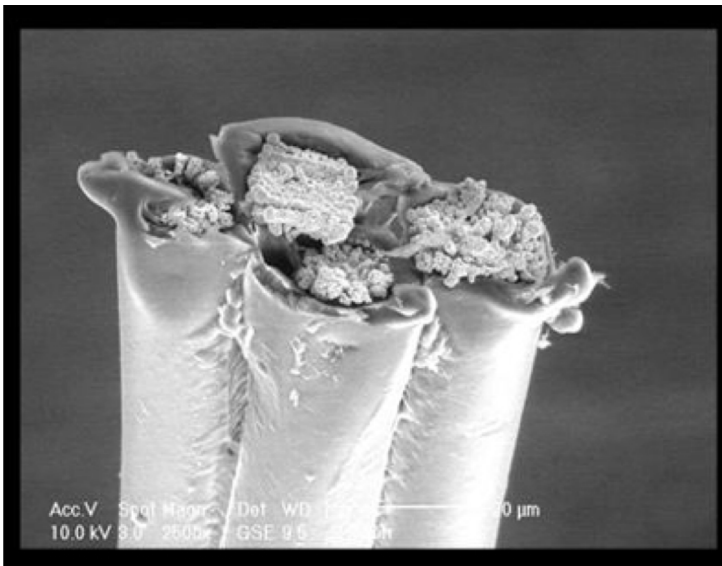
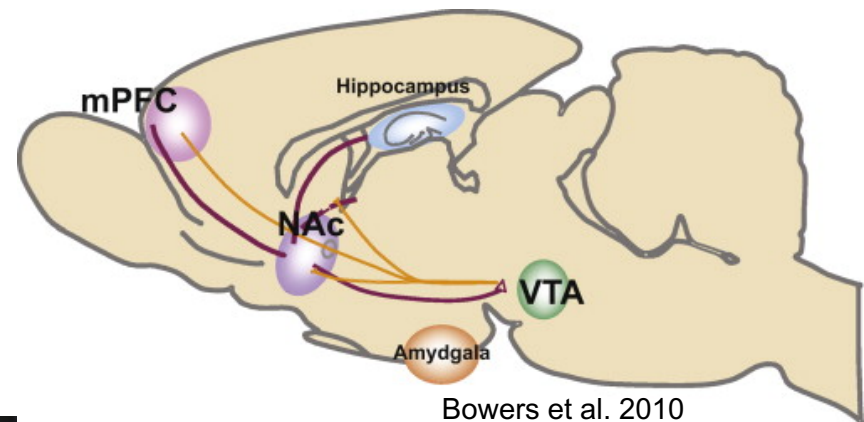
- "... a peculiar anaesthetic state in which marked sensory loss and analgesia as well as amnesia is not accompanied by actual loss of consciousness." (Bonta, 2004)

Subanaesthetic Doses:

- Model of psychosis in animals, producing hyperlocomotion and disruption of PPI
- Reproduces in humans both positive and negative symptoms of schizophrenia along with associated cognitive deficits.

The Ketamine Model of Psychosis & Schizophrenia

With Matthew Jones, University of Bristol



Ketamine Dose: 0, 2, 4, 8, 30 mgkg⁻¹

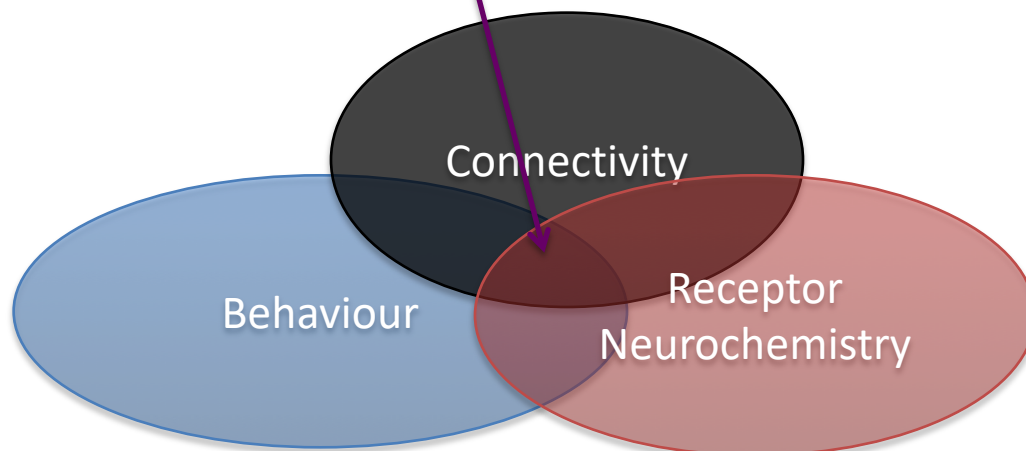
Hippocampal & Prefrontal Recordings

5 mins of recordings from freely moving rat: tetrodes in dCA1 & mPFC

The Ketamine Model of Psychosis & Schizophrenia

Effects on Oscillations:

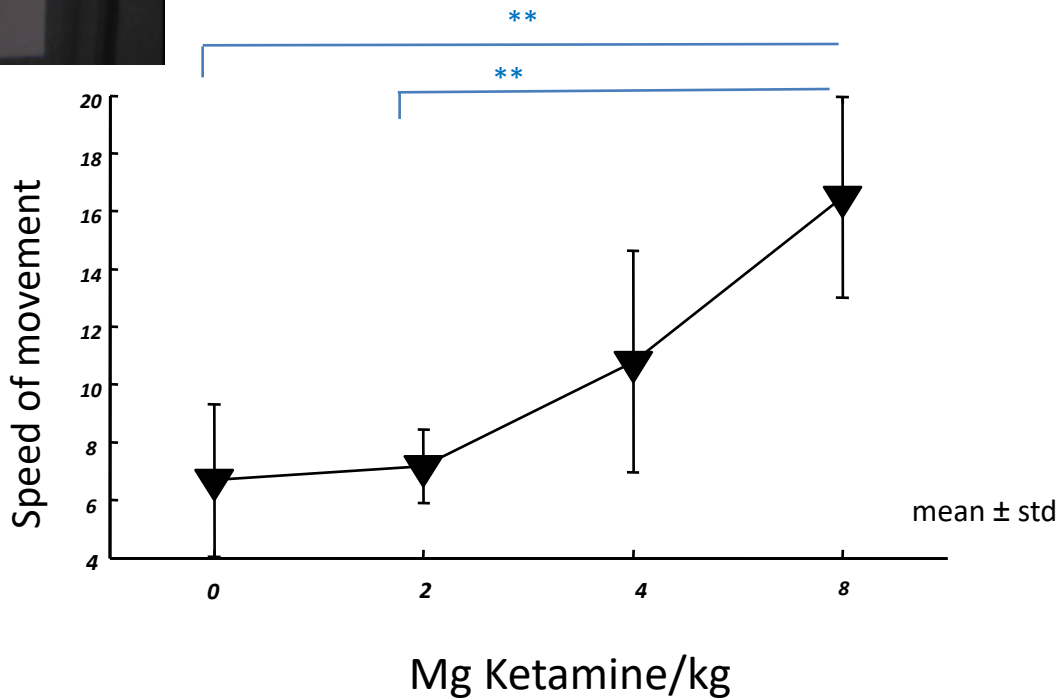
- Theta reduction in the hippocampus and Gamma enhancement in hippocampus and neocortex.
- Antipsychotic drugs (D2 antagonists) acutely reduce cortical gamma oscillations in rats (Jones et al. 2011).
- Aberrant beta and gamma synchrony observed in patient populations (Uhlhaas et al. 2008).
- Reduced or enhanced gamma depending on state late/prodromal (Sun et al. 2011).



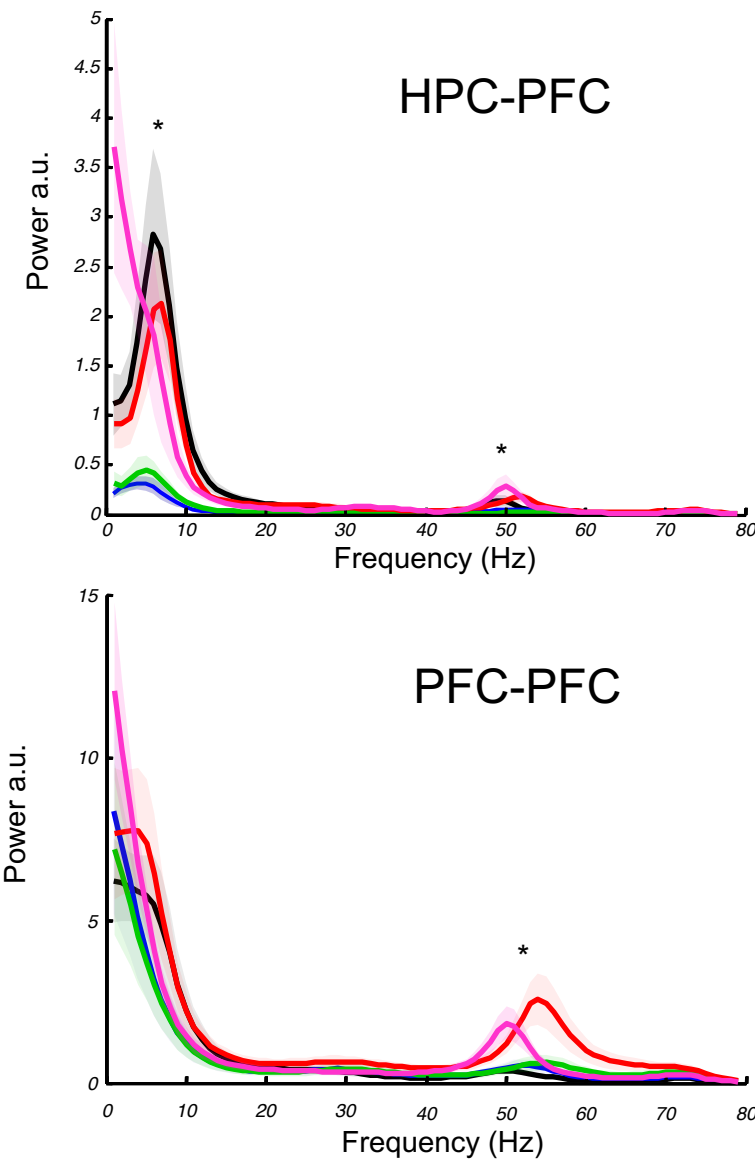
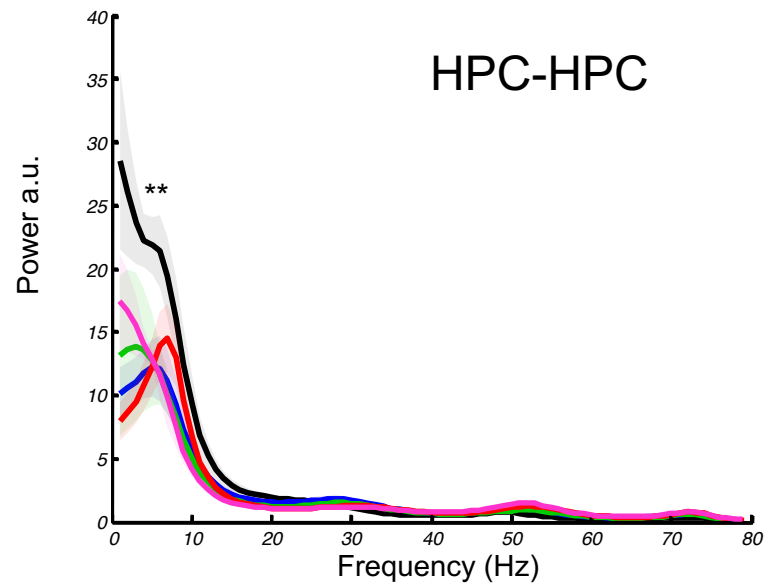
Behavioural Phenotype



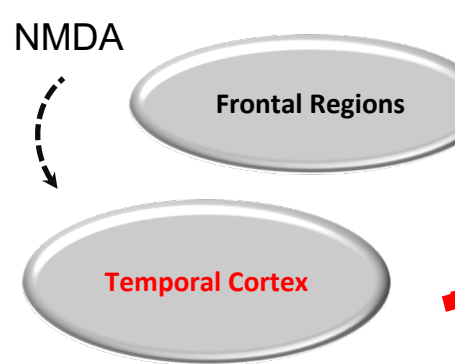
Hyper-locomotion



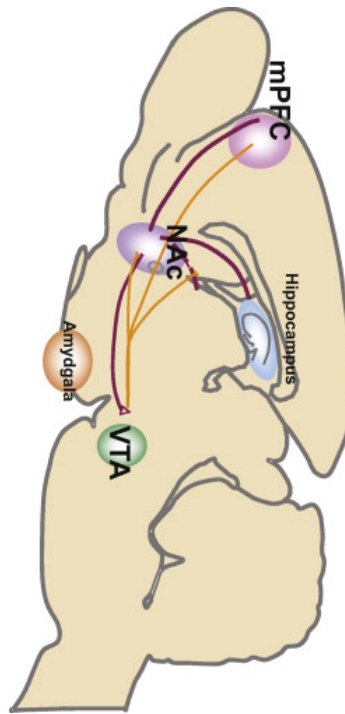
Oscillatory Characteristics



Hypothesis, Data & Model-based analysis:



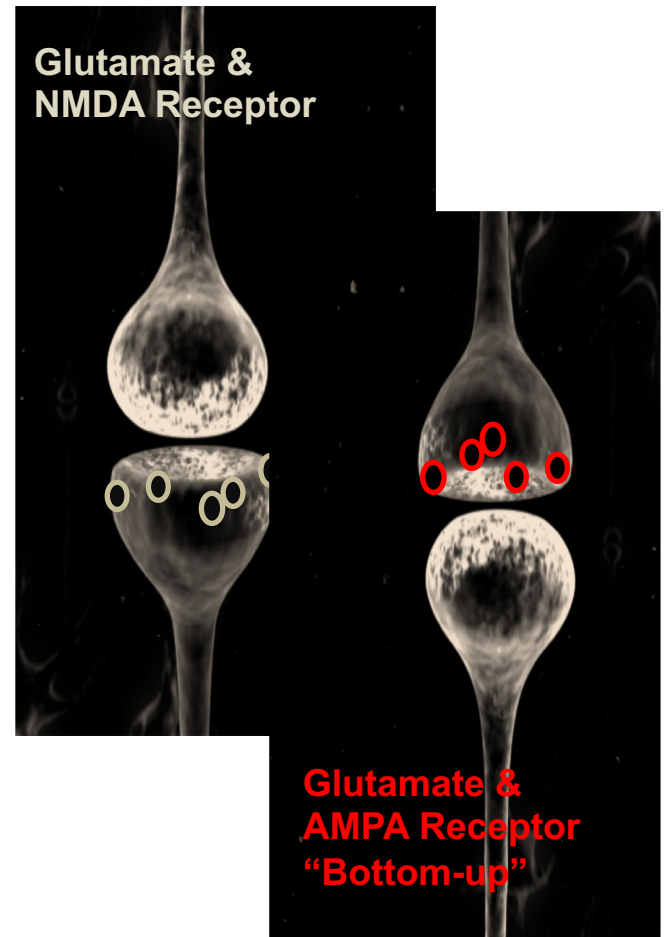
Dopamine
Gamma
Gaba



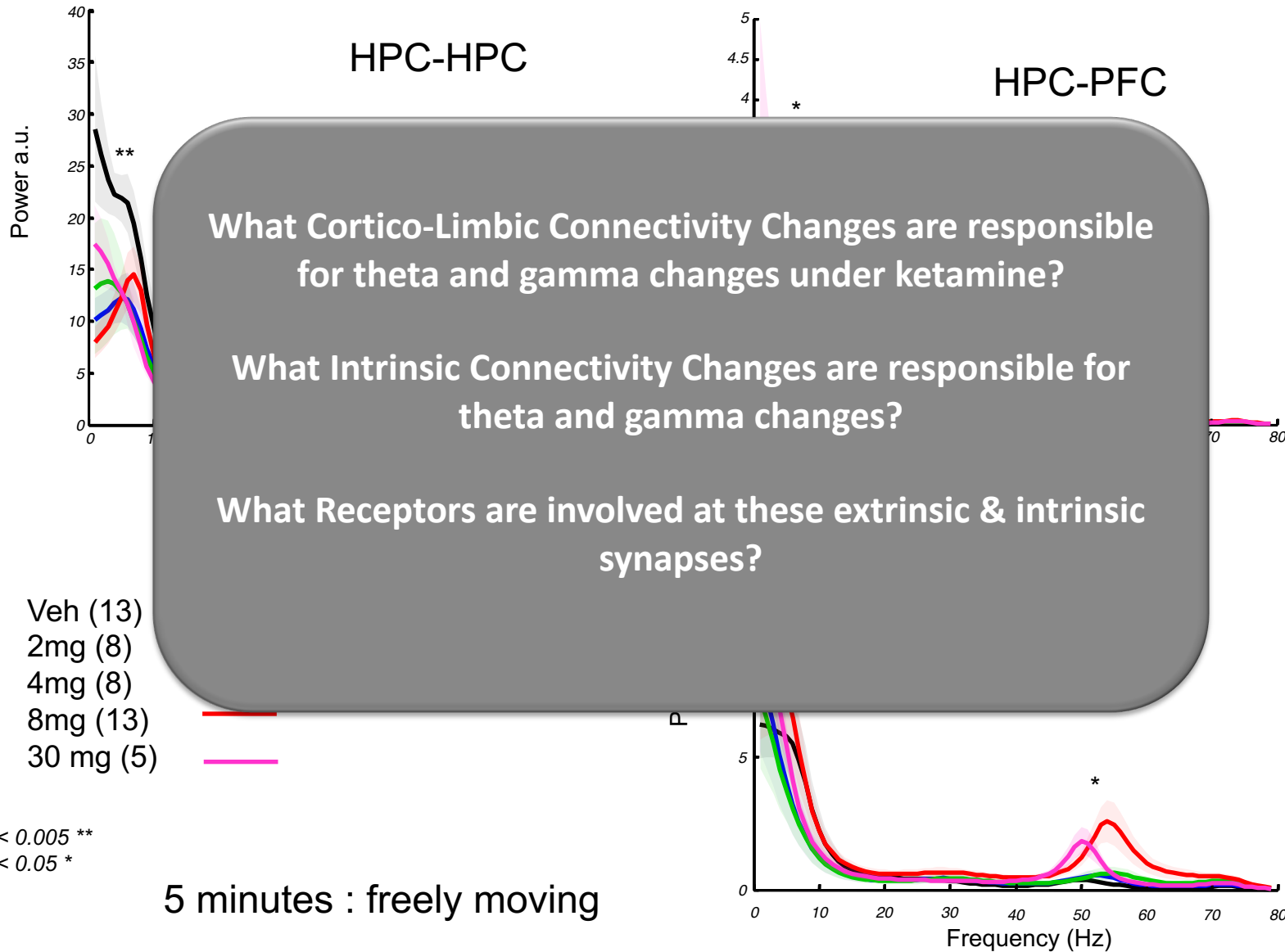
Hippocampal & Prefrontal Recordings

5 mins of recordings from freely moving rat: tetrodes in dCA1 & mPFC

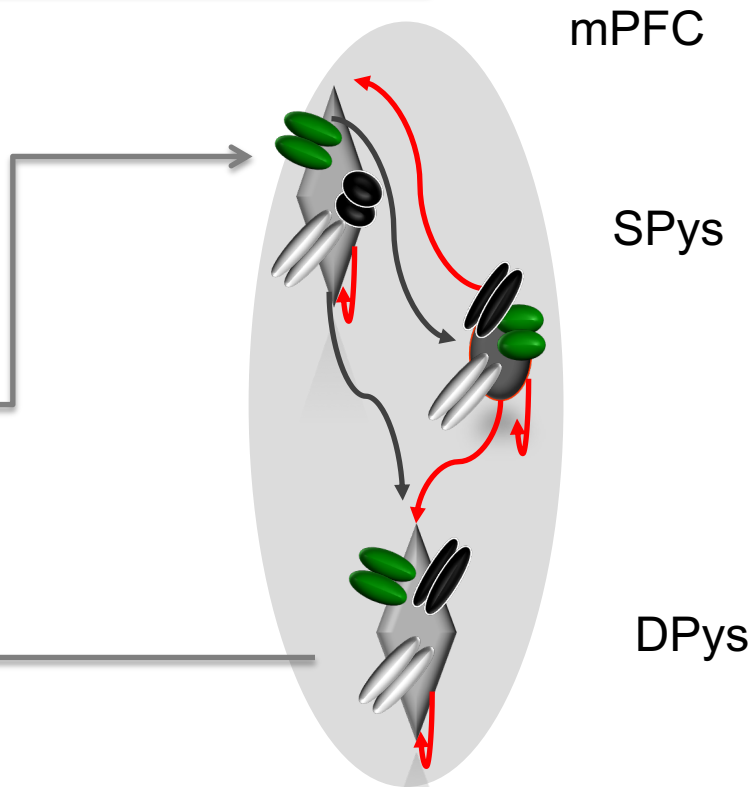
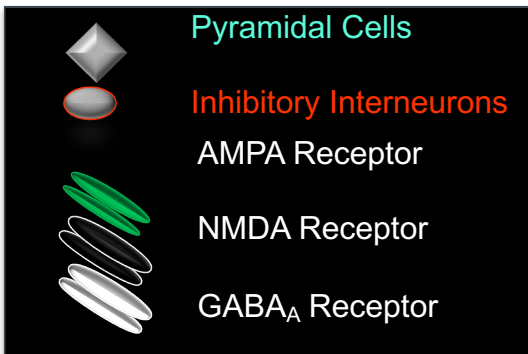
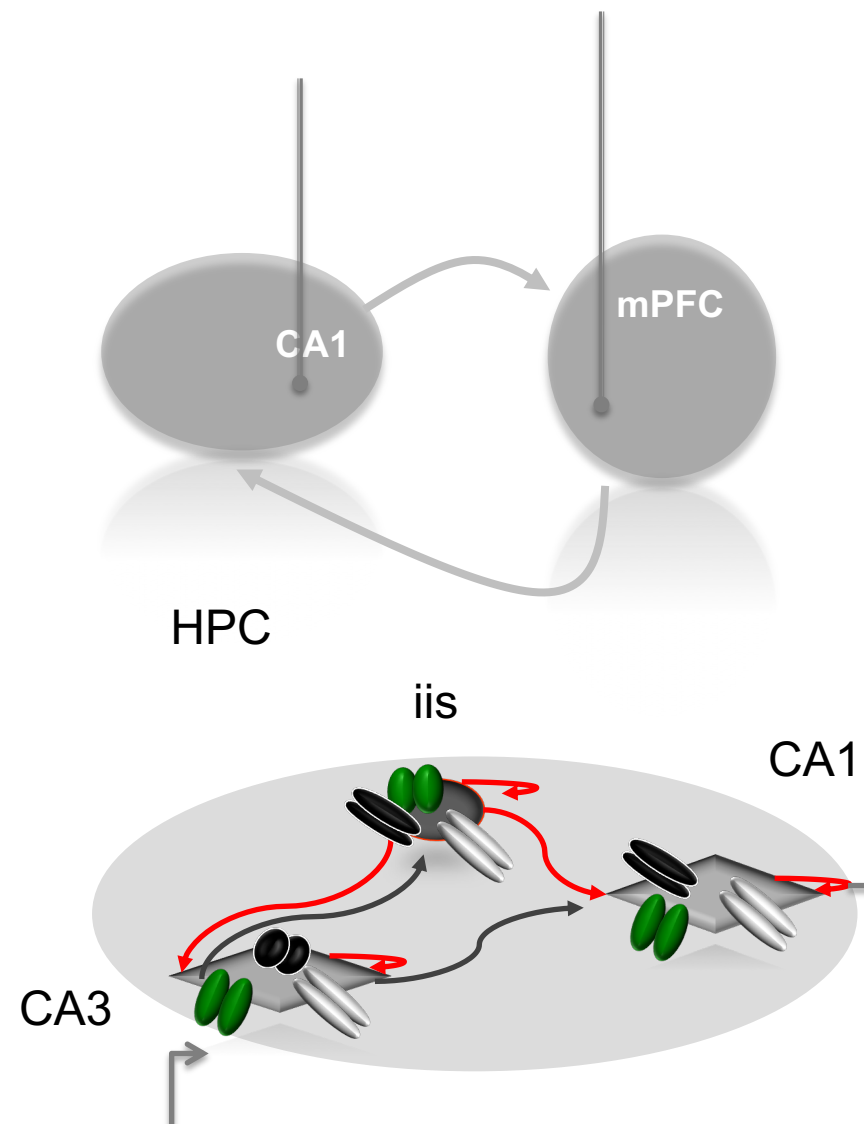
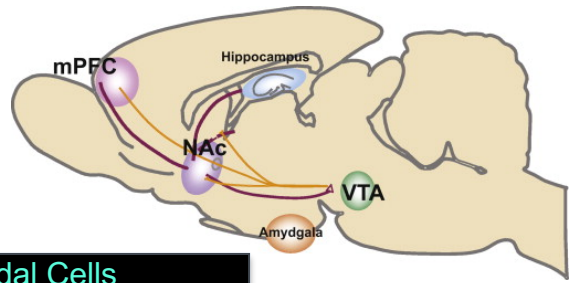
Ketamine Dose: 0, 2, 4, 8, 30 mgkg⁻¹



Hypothesis, Data & Model-based analysis:



Proposed Architecture

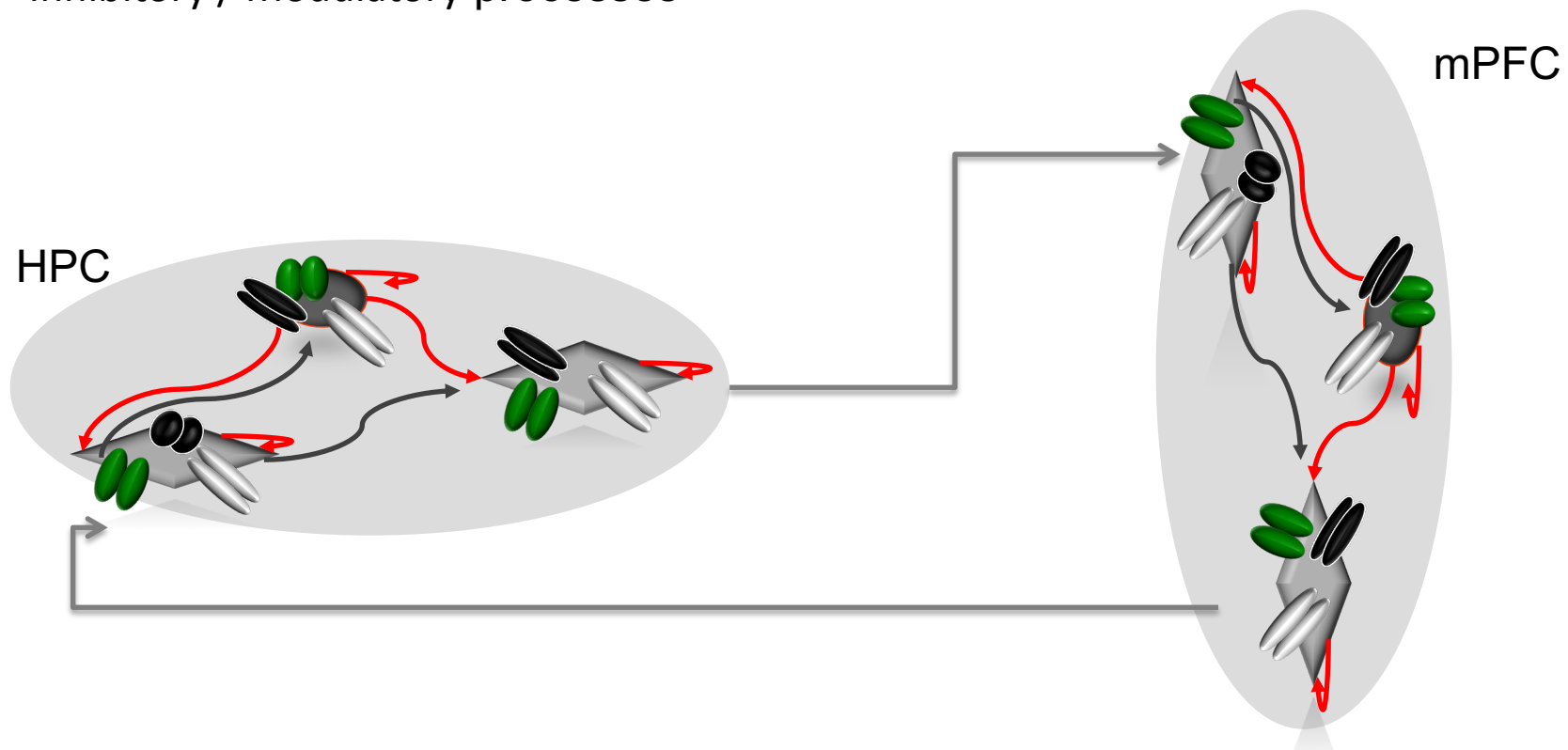


Model Comparison

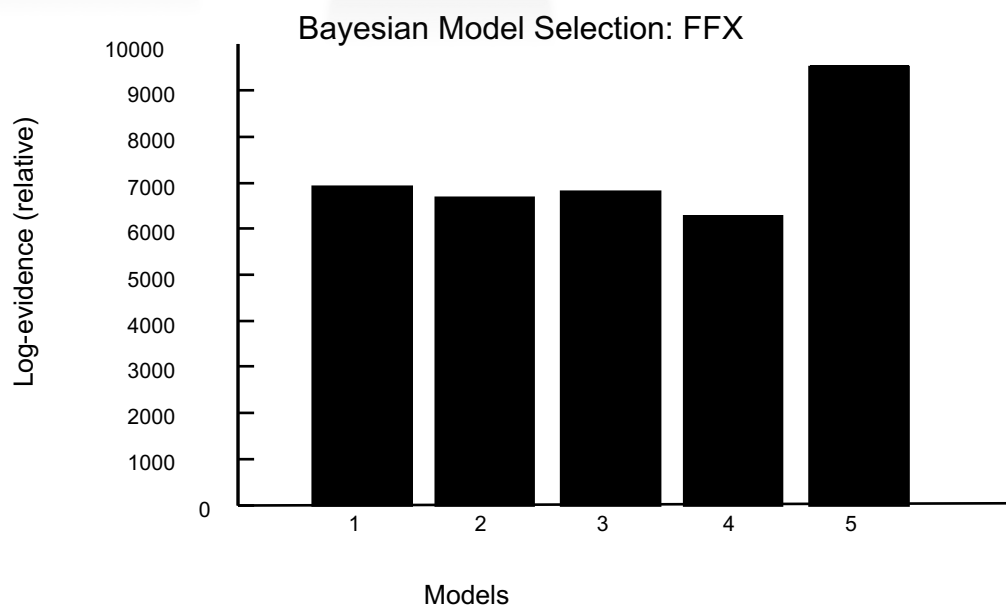
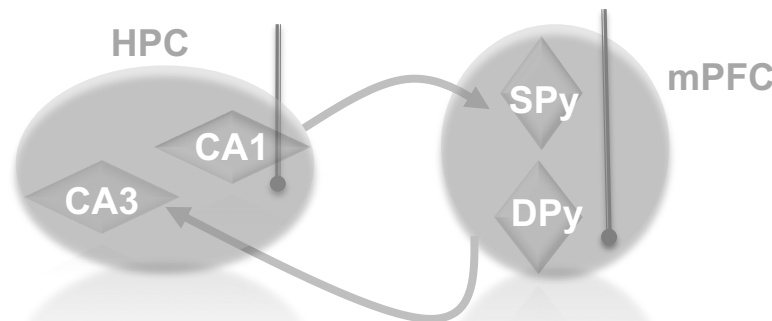
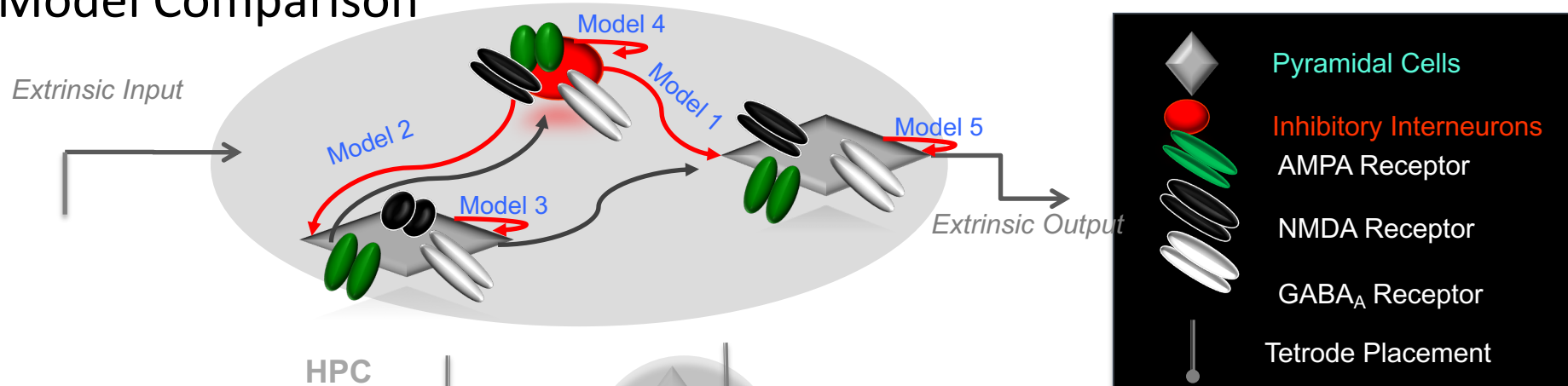
Ketamine doses parametrically modulate:

1. All extrinsic connections,
2. Intrinsic NMDA and
3. Inhibitory / Modulatory processes

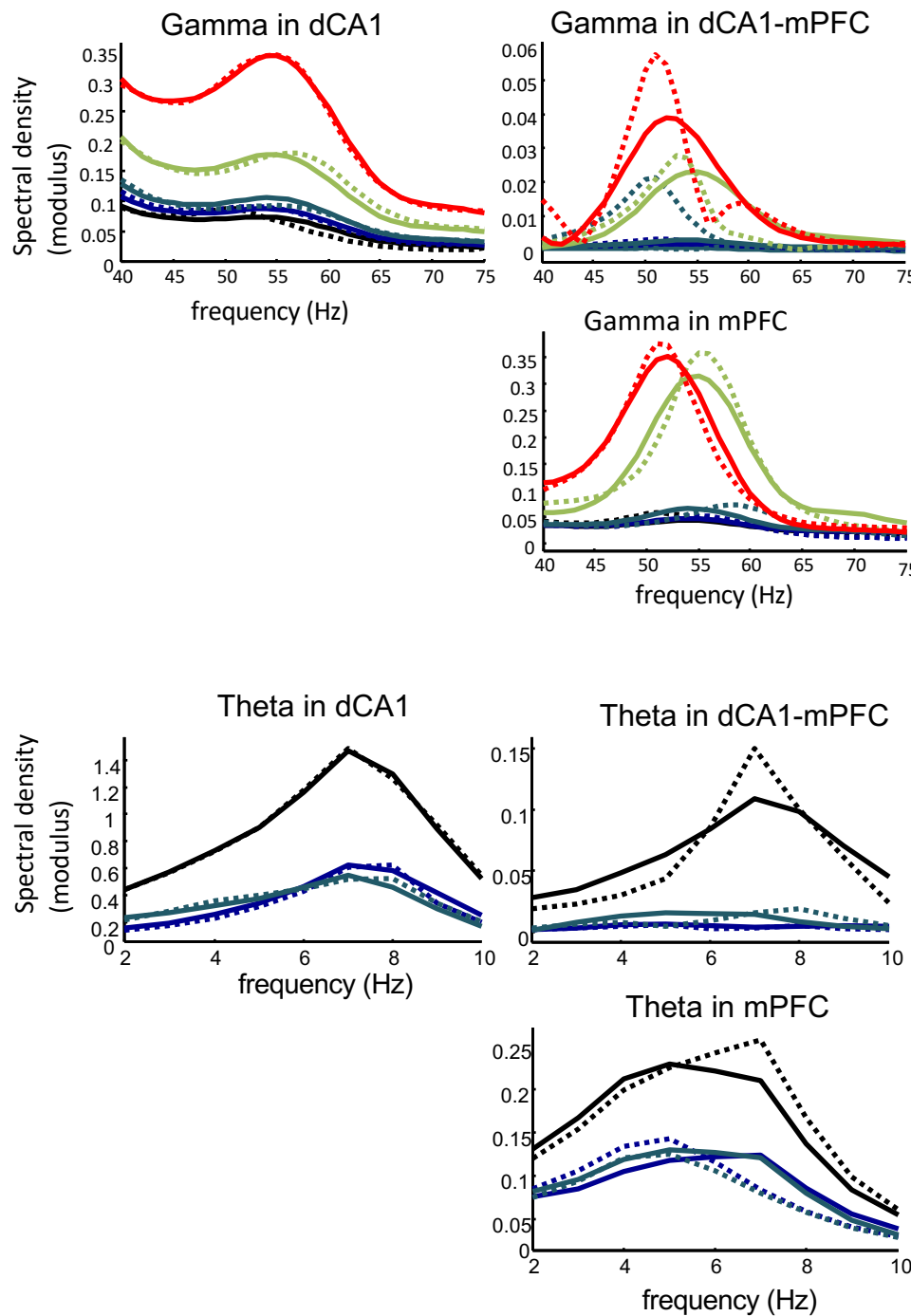
$$\gamma = \gamma + B_{ket}\gamma$$



Model Comparison

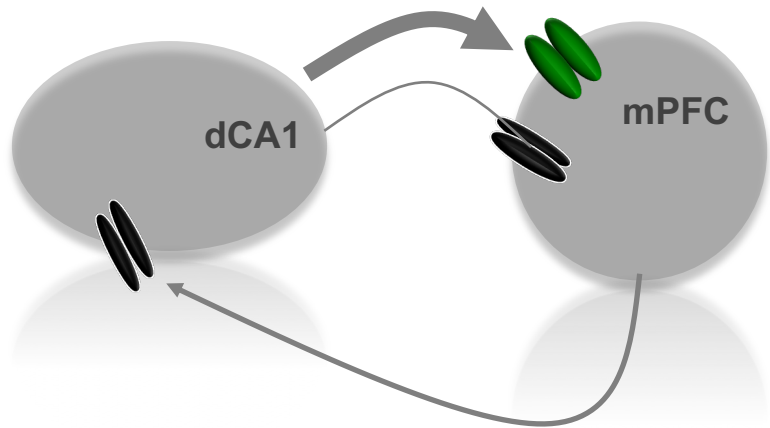


Model Fits



- predicted: saline vehicle
- observed: saline vehicle
- predicted: 2 mgkg^{-1}
- observed: 2 mgkg^{-1}
- predicted: 4 mgkg^{-1}
- observed: 4 mgkg^{-1}
- observed: 8 mgkg^{-1}
- observed: 8 mgkg^{-1}
- predicted: 30 mgkg^{-1}
- observed: 30 mgkg^{-1}

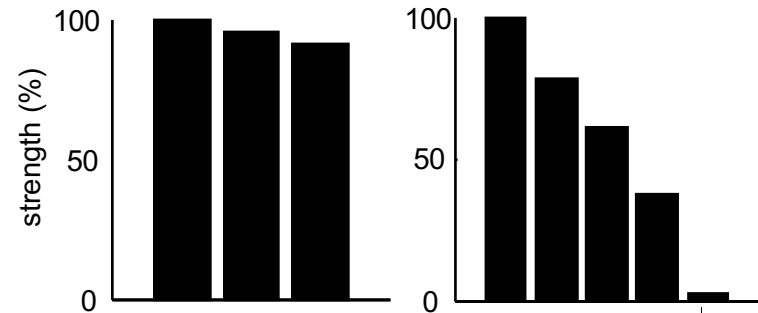
Extrinsic Connectivity Changes under Ketamine



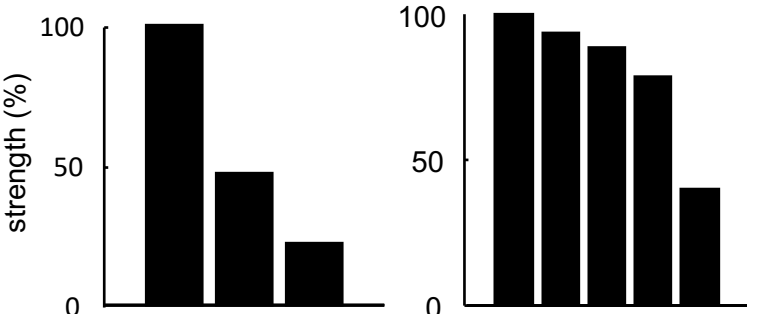
Theta Model

Gamma Model

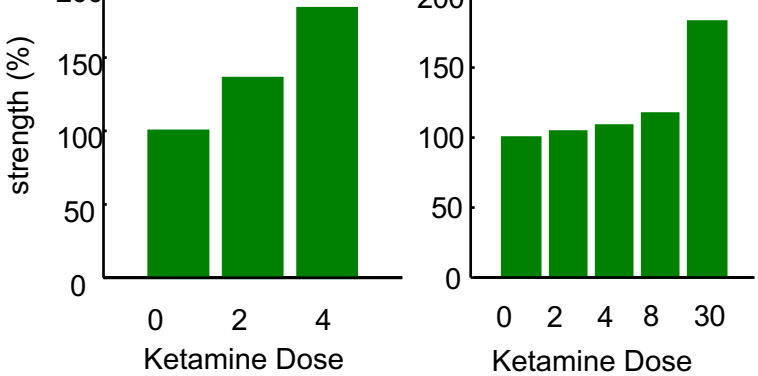
NMDA-mediated input to HPC from mPFC



NMDA-mediated input to PFC from dCA1

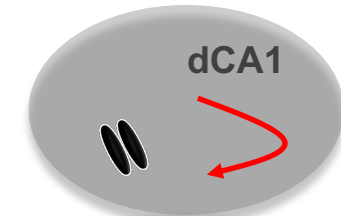


AMPA-mediated input to PFC from dCA1



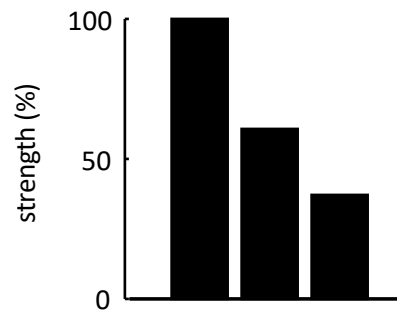
Intrinsic Connectivity Changes under Ketamine

Confirmed by MUA in CA1:
High but uncorrelated unit activity

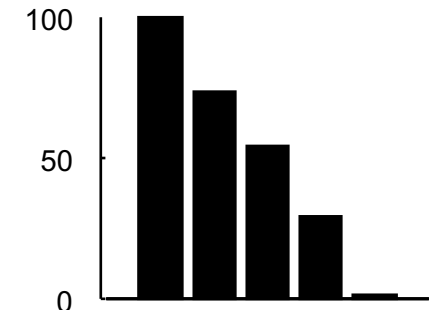


Theta Model

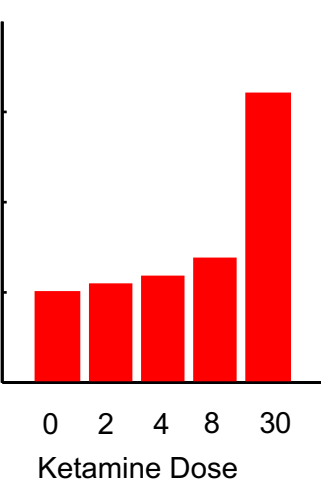
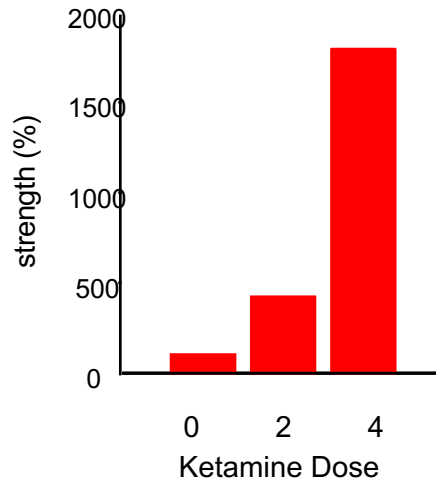
NMDA-mediated excitation of hippocampal Interneurons



Gamma Model

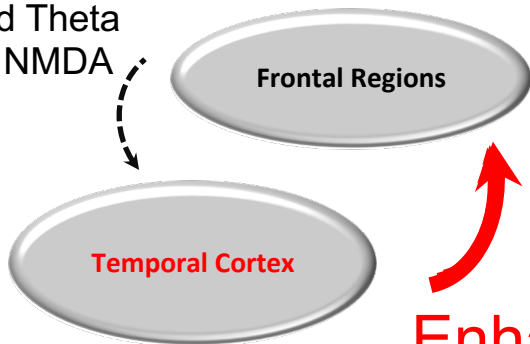


1/Signal to Noise Ratio in the Hippocampus



Losing Control Under Ketamine

Reduced Theta
Without NMDA



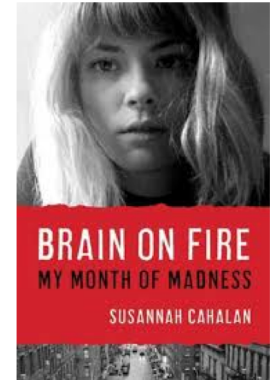
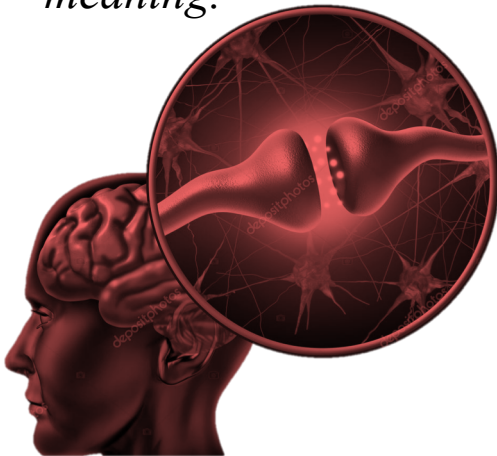
Enhanced Gamma
With AMPA

- Reduced Cortico-Limbic Control mediated by NMDA
- Enhanced Limbic-Cortico Drive via AMPA:
- Runaway bottom-up sensory-driven processing : disorganised cognition & environmental interactions
- Large difference in intrinsic processing: early dopaminergic D2 problem in schizophrenia?

DCM of Human EEG Data in Psychosis-related Autoimmune Disease

DCM of Human EEG Data in Psychosis-related Autoimmune Disease

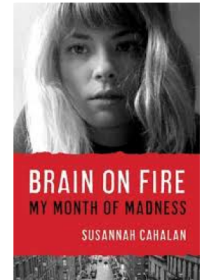
“I was walking through Times Square, during which colors appeared aggressively bright. I remember thinking: “I’m seeing everything in a sinister light now. Everything is dripping in terrible meaning.”



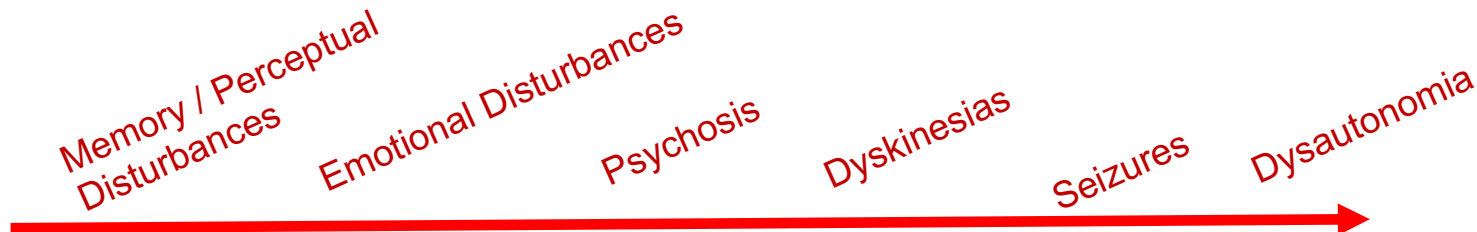
“In the spring of 2009, I was the 217th person ever to be diagnosed with anti-NMDA-receptor autoimmune encephalitis. Just a year later, that figure had doubled. Now the number is in the thousands. Yet Dr. Bailey, considered one of the best neurologists in the country, had never heard of it.”

Anti-NMDA Receptor Encephalitis

- “A severe, multistage, treatable disorder presenting with psychosis” (Wandinger, Dalmua, 2011)
- Autoimmune disorder – including a paraneoplastic syndrome from teratoma or other tumors
- Autoantibodies attenuate NMDAR function through the internalization of NMDAR



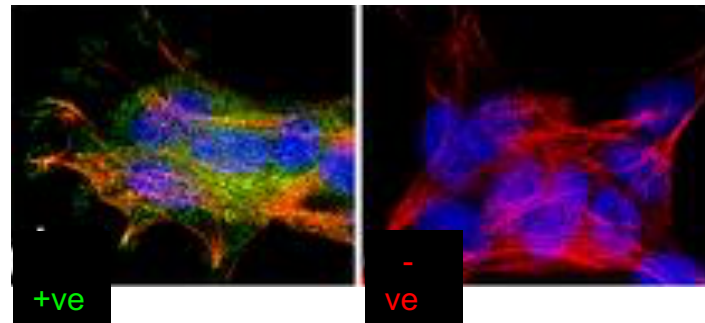
Symptoms



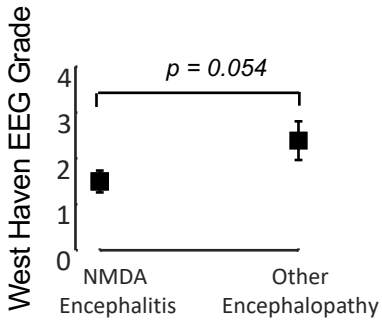
Diagnosis: A positive antibody titer

Treatment: Tumor removal, intravenous corticosteroids and intravenous immunoglobulins

Prognosis: 75% Recovery, 6 – 25% mortality

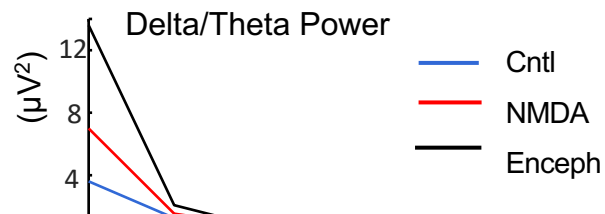
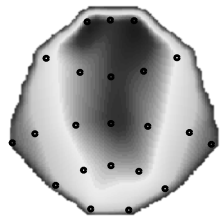


Anti-NMDA Receptor Encephalitis: Reduced Connectivity at NMDA receptors

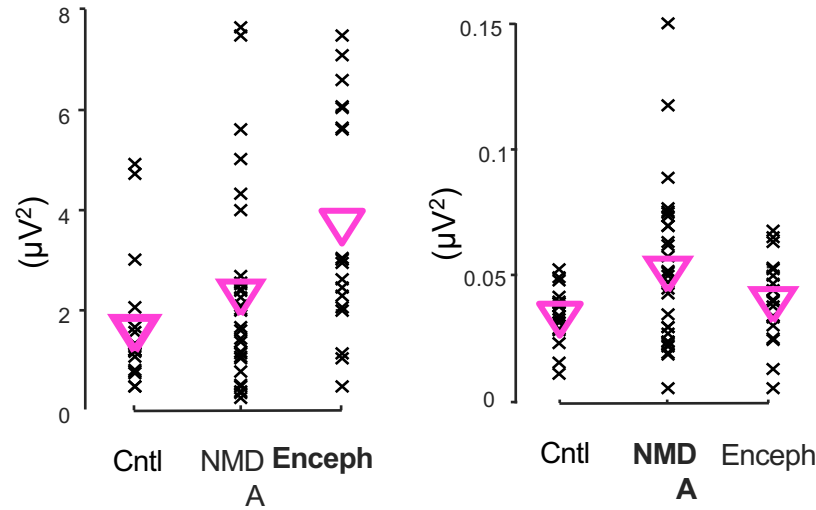
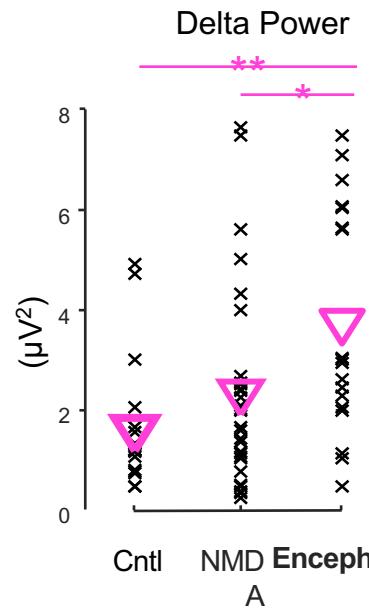
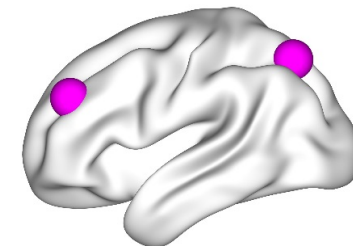
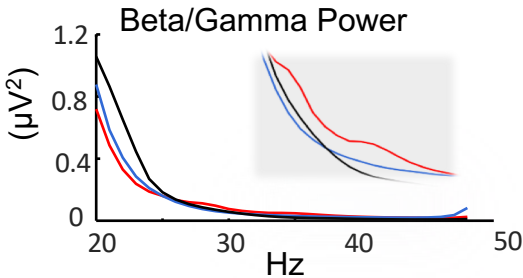
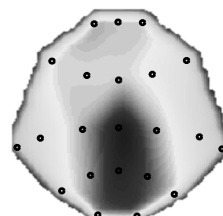
Anti-NMDA Receptor Encephalitis	Encephalopathy (Brain slowing)	Neurological Patient Controls										
+ve Serum titer												
N = 31, Age 28 yrs +/- 16, (22 Female)	N = 18, Age 28 +/- 5, (11 Female)	N = 18, Age 31 +/- 6, (10 Female)	 <p>A box plot comparing the West Haven EEG Grade between two groups. The y-axis ranges from 0 to 4. The 'NMDA Encephalitis' group has a median grade of approximately 1.5, while the 'Other Encephalopathy' group has a median grade of approximately 2.5. A horizontal bracket spans the range of the 'Other Encephalopathy' group, with a p-value of 0.054 indicated above it.</p> <table border="1"> <caption>Data from West Haven EEG Grade box plot</caption> <thead> <tr> <th>Group</th> <th>Median</th> <th>Range</th> </tr> </thead> <tbody> <tr> <td>NMDA Encephalitis</td> <td>~1.5</td> <td>0 - 3</td> </tr> <tr> <td>Other Encephalopathy</td> <td>~2.5</td> <td>2 - 3</td> </tr> </tbody> </table>	Group	Median	Range	NMDA Encephalitis	~1.5	0 - 3	Other Encephalopathy	~2.5	2 - 3
Group	Median	Range										
NMDA Encephalitis	~1.5	0 - 3										
Other Encephalopathy	~2.5	2 - 3										
12 minutes Resting State 32-channel EEG	12 minutes Resting State 32-channel EEG	12 minutes Resting State 32-channel EEG	EEGs indistinguishable on clinical inspection									
Acute, Subacute Recovering or Chronic	Etiology: Metabolic, Infectious & Hypoxic Cause		 <p>A photograph of a modern hospital building with a curved glass facade and illuminated windows, taken at night.</p>									
Treatment: steroids, plasma exchange, IVG												

Anti-NMDA Receptor Encephalitis: Spectral Responses

Power (2-6 Hz)



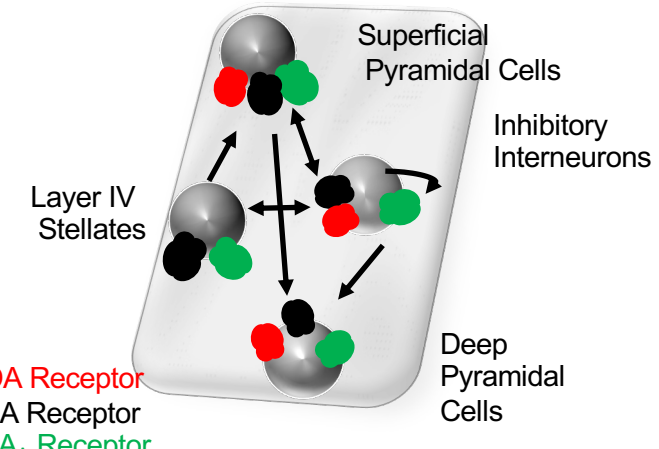
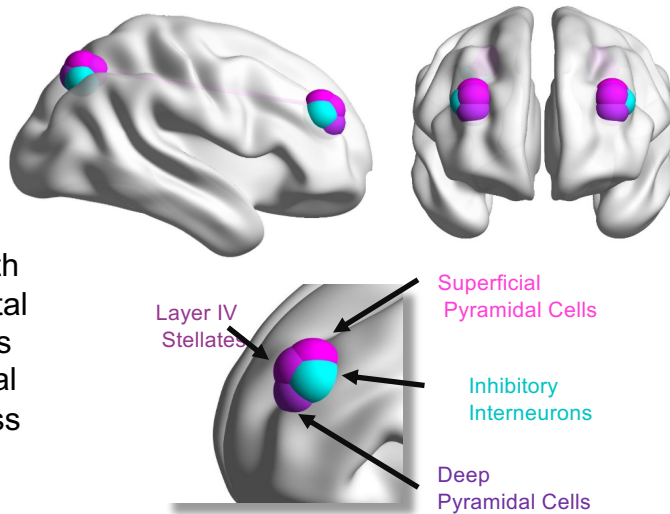
Power (20-48 Hz)



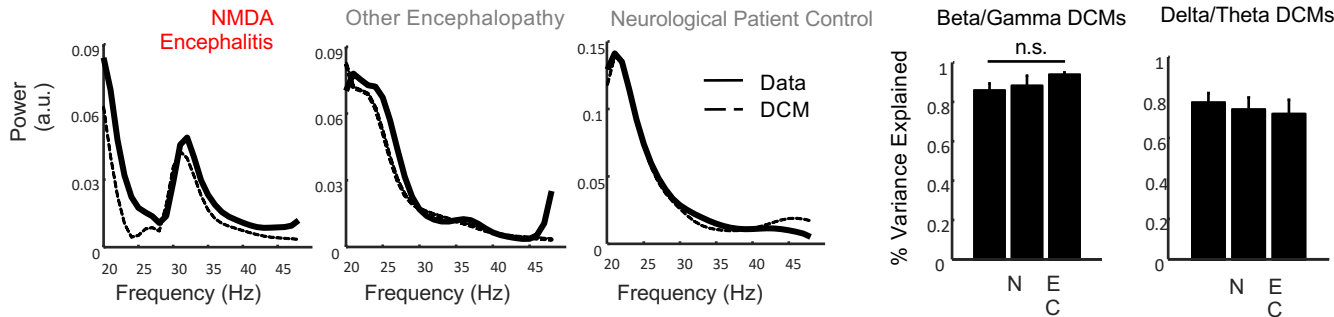
DCM: Anti-NMDA Receptor Encephalitis

Neural Mass Model's Intrinsic Connectivity

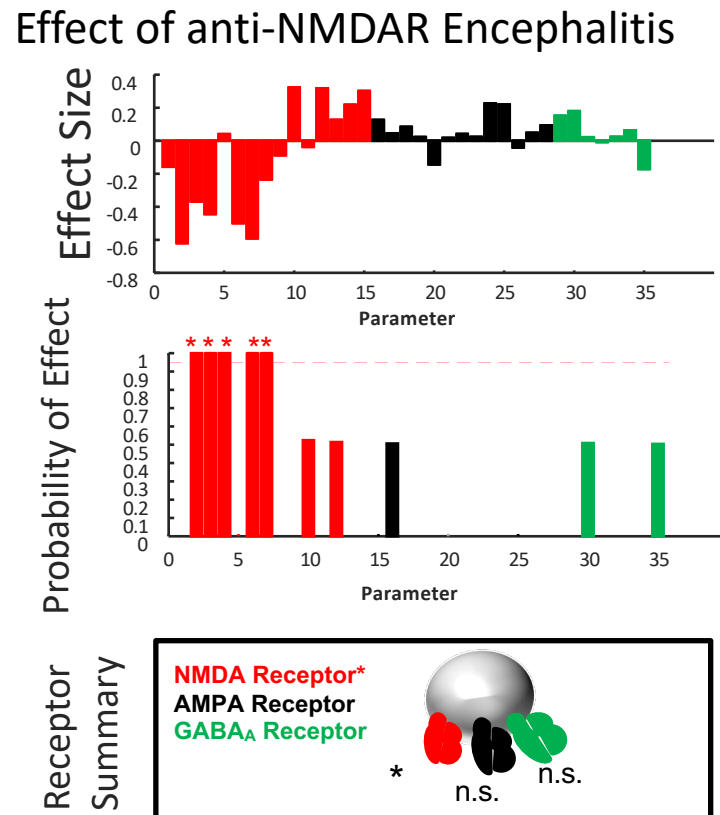
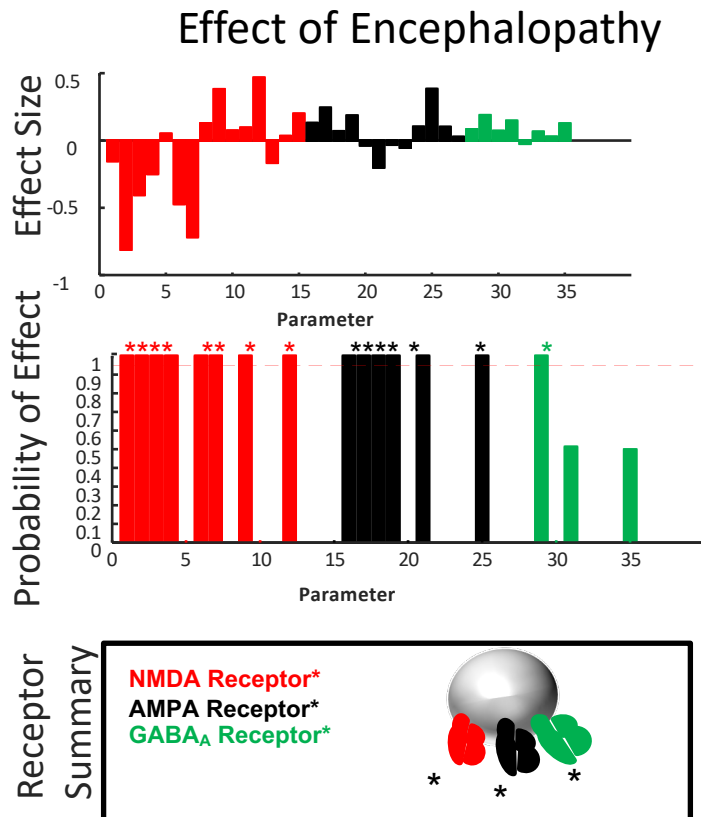
Bilateral network with frontoparietal connections and regional Neural Mass Models



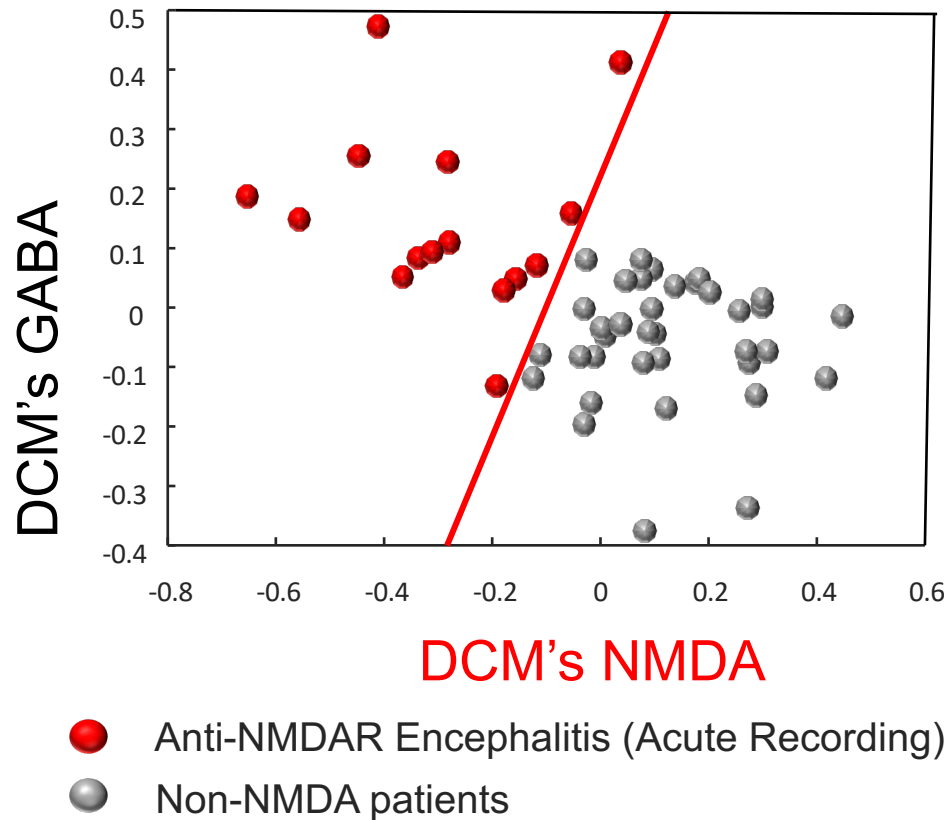
Model Fits



Group Effects (PEB)

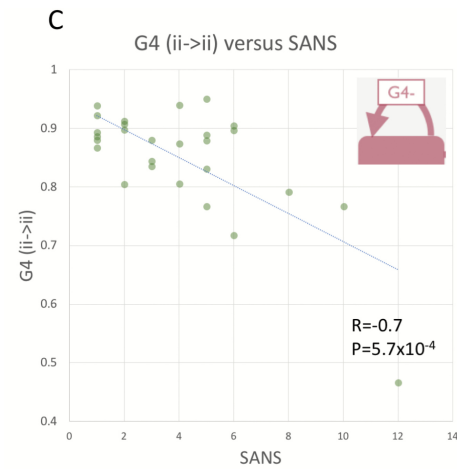
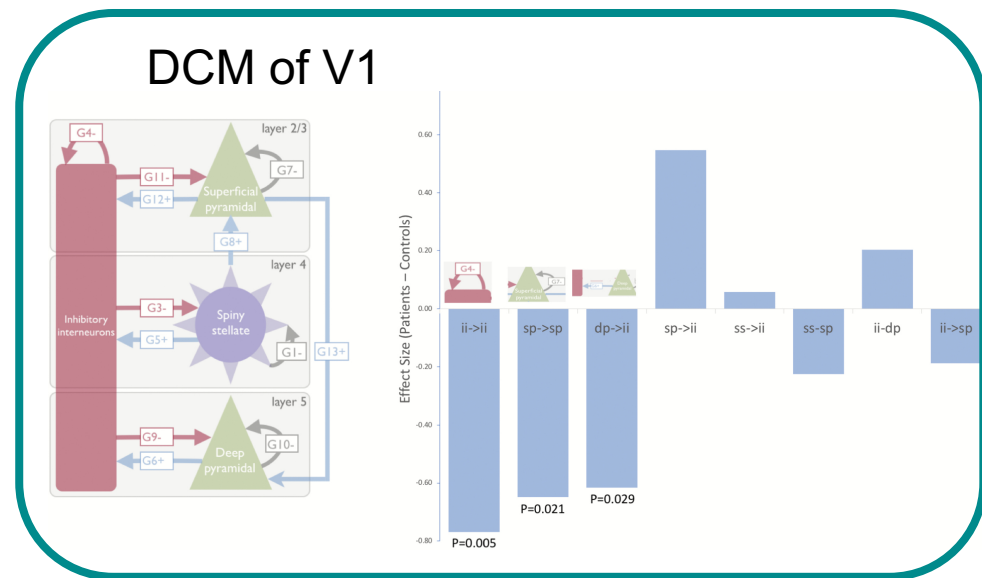
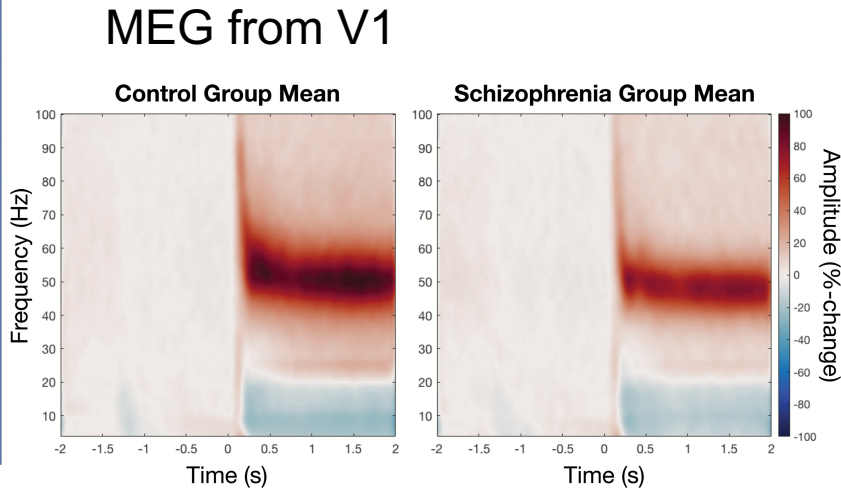
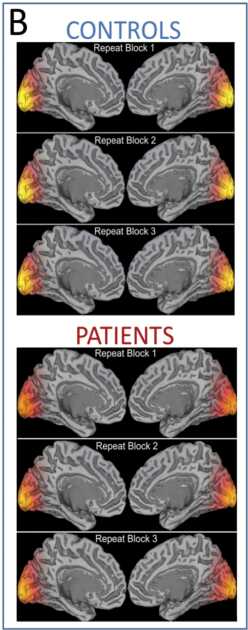
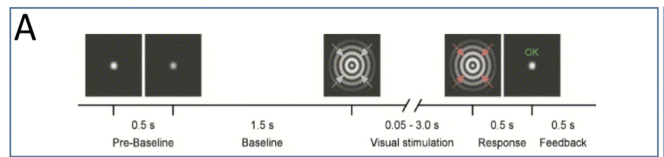


Receptor Phenotyping using EEG



Symmonds et al. *Brain* 2018

Receptors & Behaviour through MEG



Shaw et al. 2020

GABA to GABA

Schizophrenia, Brain Connectivity Towards Genetics

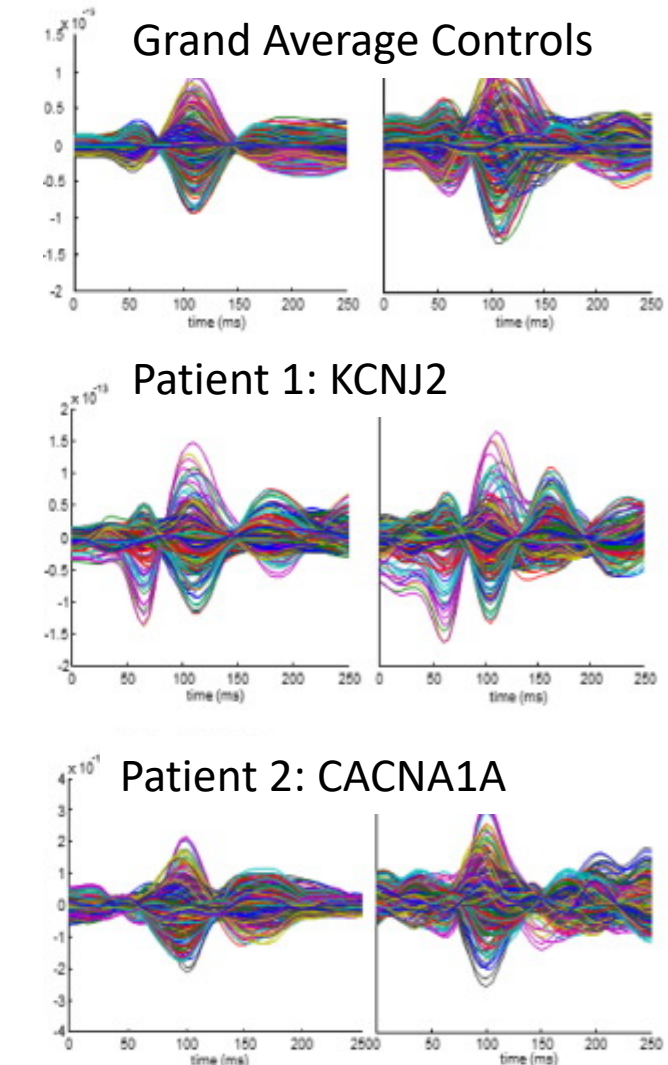
Channelopathies : genetic mutations

leading to gain or loss of function 'knock-outs'

Aim: Identify channel abnormality in 2 patients with genetic mutations causing loss-of-function in the inward-rectifying potassium channel gene KCNJ2 (Andersen-Tawil Syndrome) and in the voltage-gated presynaptic calcium channel gene CACNA1A (Episodic Ataxia Type 2)



Gilbert et al. 2016



Schizophrenia, Brain Connectivity Towards Genetics

Channelopathies : genetic mutations

leading to gain or loss of function 'knock-outs'

Aim: Identify channel abnormality in 2 patients with genetic mutations causing loss-of-function in the inward-rectifying potassium channel gene KCNJ2 (Andersen-Tawil Syndrome) and in the voltage-gated presynaptic calcium channel gene CACNA1A (Episodic Ataxia Type 2)

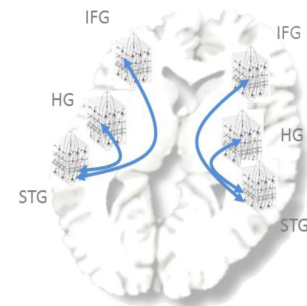
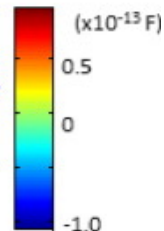
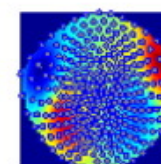
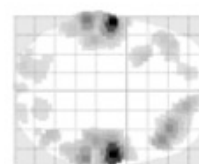
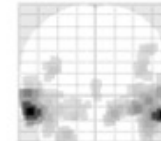
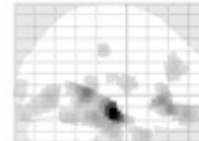


Gilbert et al. 2016

Patient 2:

CACNA1A

Standard



Schizophrenia, Brain Connectivity Towards Genetics

Channelopathies : genetic mutations

leading to gain or loss of function 'knock-outs'

Aim: Identify channel abnormality in 2

patients with genetic mutations causing
loss-of-function in the inward-rectifying
potassium channel gene KCNJ2

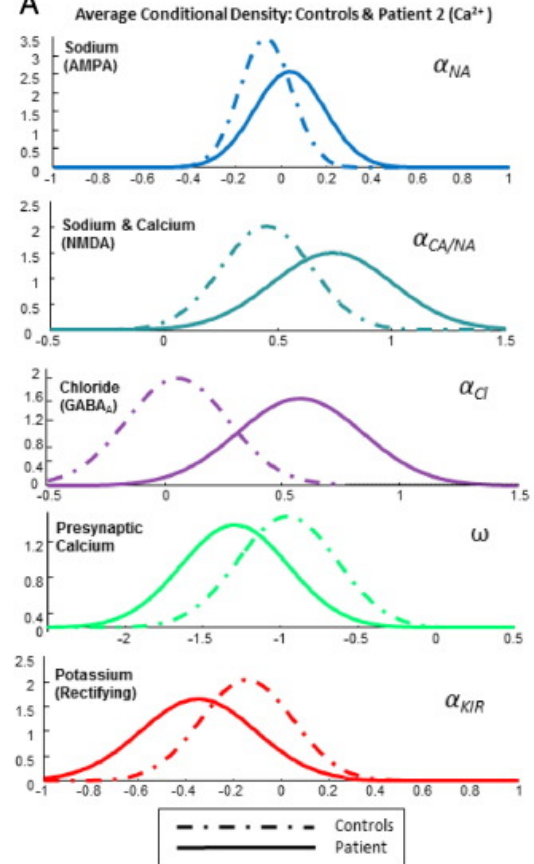
(Andersen-Tawil Syndrome) and in the
voltage-gated presynaptic calcium
channel gene CACNA1A (Episodic Ataxia
Type 2)



Gilbert et al. 2016

Controls vs Patient 2 CACNA1A

A



Why these models?

DCM for EEG

Why I think these models are useful:

Models of Synaptic Activity using invasive and non-invasive electrophysiological time series from large neuronal populations.

Useful models of pharmacological effects – where are the drug's effects most prominent, are other receptors affected?

Useful link to predictive coding: top-down vs. bottom up and their belief mappings.

Potential to scale to clinical settings: could patients be stratified based on endogenous connectivity profiles?

DCM for EEG

Why these models can be more than mildly irritating :

Local Minima (not the model's fault)



Thank You

TNU & The FIL Methods Group